HHS Public Access

Author manuscript

Exp Eye Res. Author manuscript; available in PMC 2016 December 01.

Published in final edited form as:

Exp Eye Res. 2015 December ; 141: 57–73. doi:10.1016/j.exer.2015.06.005.

The Non-Human Primate Experimental Glaucoma Model

Claude F. Burgoyne

Devers Eye Institute, Optic Nerve Head Research Laboratory, Legacy Health System, Portland, Oregon

Abstract

The purpose of this report is to summarize the current strengths and weaknesses of the non-human primate (NHP) experimental glaucoma (EG) model through sections devoted to its history, methods, important findings, alternative optic neuropathy models and future directions. NHP EG has become well established for studying human glaucoma in part because the NHP optic nerve head (ONH) shares a close anatomic association with the human ONH and because it provides the only means of systematically studying the very earliest visual system responses to chronic IOP elevation, i.e. the conversion from ocular hypertension to glaucomatous damage. However, NHPs are impractical for studies that require large animal numbers, demonstrate spontaneous glaucoma only rarely, do not currently provide a model of the neuropathy at normal levels of IOP, and cannot easily be genetically manipulated, except through tissue-specific, viral vectors. The goal of this summary is to direct NHP EG and non-NHP EG investigators to the previous, current and future accomplishment of clinically relevant knowledge in this model.

Keywords

Non-human primate; Monkey; Glaucoma; Experimental Glaucoma; Optic Nerve Head; Optic Nerve; Sclera; Retina; Remodeling

Introduction

While varying forms of chronic experimental intraocular pressure (IOP) elevation were reported in the non-human primate (NHP) by a series of investigators beginning in the late

Corresponding Author: Claude F. Burgoyne, MD, Devers Eye Institute, Optic Nerve Head Research Laboratory, Discoveries in Sight Research Laboratories, Legacy Research Institute, 1225 NE 2nd Ave, Portland OR 97232. cfburgoyne@deverseye.org. Tel: +1-503-413-5441, Fax: +1-503-413-5179.

Disclosures While not directly involved in the creation of this manuscript, important conversations over the past 24 years with a large group of mentors, investigators, collaborators, colleagues, post-docs and students have shaped my understanding of NHP EG. These include but are not limited to Harry Quigley, Doug Anderson, Don Zack, Rob Nickells, Mary Ellen Pease, Rosario Hernandez, Don Minckler, Ran Zeimer, Rich Hart, Francis Suh, Hilary Thompson, Crawford Downs, Anthony Bellezza, Ian Sigal, Michael Girard, Ross Ethier, John Flanagan, Elke Lutjen-Drecoll, Hongli Yang, Juan Reynaud, Howard Lockwood, Nick Strouthidis, Kevin Ivers, Jonathan He, Jason Porter, Camila Zangalli, Jack Cioffi, Mike Van Buskirk, Brad Fortune, Lin Wang, Stuart Gardiner, Cheri Stowell, John Crabb, Nick Marsh-Armstrong, Gareth Howell, Simon John, Abe Clark, John Morrison, Elaine Johnson, Ron Harwerth, Chris Girkin, Paul Kaufman, Bal Chauhan and Gerhard Zinser.

1950s and early1960s, the first description of the current model of chronic, laser-induced, unilateral IOP elevation is generally ascribed to a 1974 publication by Gasterland and Kupfer (Gaasterland and Kupfer, 1974). During the ensuing 40 years, the NHP experimental glaucoma (EG) model has become well established for studying human glaucoma in part because the NHP optic nerve head (ONH) shares a close anatomic association with the human ONH and in part because this association is consistent throughout each component of the visual system. The model is also important because it provides the only means of systematically studying the very earliest visual system responses to chronic IOP elevation, i.e. the conversion from ocular hypertension to glaucomatous damage. Human eyes at this stage of "damage" cannot be clinically recognized nor can they be expected to occur in subjects who are close to death (i.e close to post-mortem, tissue donation). However, NHPs are impractical for studies that require large animal numbers, demonstrate spontaneous glaucoma only rarely, do not currently provide a model of the neuropathy at normal levels of IOP, and cannot easily be genetically manipulated, except through tissue-specific, viral vectors. NHP EG often occurs at levels of IOP that are higher than (Gardiner et al., 2012), and in eyes from animals that are "younger" than (Gardiner et al., 2012), most human primary open angle glaucoma (POAG) patients (Tielsch et al., 1991a; Tielsch et al., 1991b). The purpose of this report is to summarize the current strengths and weaknesses of the NHP EG model through sections devoted to its history, methods, important findings, alternative optic neuropathy models and future directions. To provide context, it starts with a review of what is known about spontaneous NHP glaucoma and other spontaneous forms of NHP optic neuropathy.

To clarify terminology within this article, "naive" normal eyes from bilateral normal animals will be referred to as "normal". The contralateral, "untreated" eye of an animal with unilateral EG will be referred to as a "control" eye and the treated eye will be referred to as the pre-EG eye during its period of baseline testing and the "EG" eye following the onset of trabecular meshwork lasering whether IOP elevation and/or the clinical onset of glaucoma has been detected or not. Glaucoma that has been recognized to be present in wild-caught NHPs will be referred to as "spontaneous" glaucoma.

Spontaneous NHP Glaucoma and Other Spontaneous NHP Optic Neuropathies

A small colony of Rhesus Macaque monkeys from the closed Cayo Santiago colony of the University of Puerto Rico, was first reported to contain animals that demonstrated ocular hypertension, an optic neuropathy progressing in the setting of ocular hypertension and the presence of ONH changes suspicious for glaucoma in the absence of detected elevated pressure in 1993 (Dawson et al., 1993). A series of subsequent reports (Dawson et al., 1998; Dawson et al., 2005; Komaromy et al., 1998; Toris et al., 2010) defined a variety of ocular and demographic characteristics of subsets of animals, but the genetics of the colony and the histologic features of the neuropathy have not yet been described. A second small group of ocular hypertensive animals has been identified within an NHP colony in Singapore. A formal description of these animals is in preparation *(verbal communication, Tina Wong).* An idiopathic bilateral optic neuropathy that demonstrated non-glaucomatous pallor of the

ONH accompanied by retinal nerve fiber layer (RNFL) thinning most predominant within the maculopapular bundle has been described in 9 NHPs of Chinese origin obtained from two different primate centers (Fortune et al., 2005). Evidence of a toxic or nutritional cause for that neuropathy could not be found.

History of the Model

A variety of agents have been employed to achieve acute and short-term IOP elevation in NHPs including alpha chymotrypsin (Hamasaki and Ellerman, 1965; Hamasaki and Fujino, 1967; Kalvin et al., 1966; Lampert et al., 1968; Lessell and Kuwabara, 1969; Levy, 1974; Zimmerman et al., 1967) and red blood cells (Quigley and Addicks, 1980a). In general, these approaches were abandoned because IOP elevations were poorly controlled, short-term, and frequently led to a loss of posterior pole visualization (Quigley and Addicks, 1980a). Following its introduction in 1974 (Gaasterland and Kupfer, 1974), a series of investigators (Quigley, Anderson, Harwerth, Kaufman, Burgoyne and others) have employed the model in their laboratories, contributing to its development and extending its application to the study of human glaucoma.

Methods

International Animal Care and Use Committee (IACUC) Approval, Animal Costs, and Tools to Follow Each Animal

While there are no standardized protocols, the scientific details of all NHP experiments must be approved by the IACUC under whose supervision the work will be performed. For investigators contemplating NHP experiments, gaining experience with the model in a lab that practices it is both recommended and often IACUC required. Having access to an NHP lab's written IACUC proposals can be extremely helpful in crafting your own. Studying any animal species to advance human understanding is a privilege society grants to medical researchers uncomfortably. This discomfort is never more acutely felt than with NHP research. Because of the ethical issues involved in their care and the costs of purchase (currently 500 to 10,000 dollars per animal, averaging 5000 dollars, depending upon age, source and research protocol exposure (in our experience) and daily (per diem) care (currently 15 dollars per animal per day in our institution)), substantial infrastructure should be in place to monitor each animal prior to the start of their study. Such infrastructure is required to be certain that each animal is sacrificed for post-mortem study (if planned) at defensible endpoints. Close endpoint monitoring is a challenge when 4, 8, 12 or more animals are under study at a given point in time. To address these concerns we and others have constructed custom, online software which allows immediate access to animal demographic, running notes and IACUC approved protocols. IOP, clinical photo, longitudinal digital imaging and testing data, which updates and displays testing results relative to baseline mean and 95% confidence intervals at the end of each session, allows for same day onset and/or progression detection. Post-mortem tissue and data storage is also managed and accessed through these systems from whole globe to each visual system tissue type, from fixation through embedding, sectioning, staining, reconstructing, segmenting and quantification.

The Implications of Origin, Age, Gender and Sub-species Differences in Study Execution and Design

While definitive studies have not yet been done for sub-species and gender, investigators need to be aware that they may need to control for these demographic variables in their work. Even though we have twice reported no detectible differences between cynomolgous and rhesus control eye ONH connective tissue architecture using 3D histomorphometry (Lockwood et al., 2015; Yang et al., 2011b), we have chosen to concentrate our work in the rhesus to remove any possible differences in species-related susceptibility from our experiments. Cynomolgus versus Rhesus differences in Multifocal Electroretinography (mfERG) responses during NHP EG have been reported (Nork et al., 2010). Less commonly used sub-species such as the squirrel and marmoset monkey will require similar evaluation to be used in combination with rhesus macaques. Age is an important risk factor for both the onset and progression of glaucomatous damage at all levels of IOP in human glaucoma (Burgoyne, 2011; Burgoyne and Downs, 2008; Downs, 2015). A series of NHP ocular age effects have been reported (see section to follow). Controlling for age should therefore be considered depending upon the hypotheses being tested. Gender differences in NHP EG phenotype and/or susceptibility have not been explicitly studied, but should also be considered.

Quarantine - Baseline – Intervention – Post-intervention – Pre-sacrifice – Sacrifice and Post-mortem Stages of Testing/Study

Most institutions require a quarantine period after animal delivery (4 weeks is common) in which the new animals are housed together in an isolation room to protect the rest of the colony from infectious disease (most commonly tuberculosis).

Once quarantine is cleared, weekly testing sessions are allowed in our institution, assuming animal health is maintained. Anesthesia protocols are commonly test-type and institution-specific – depending upon the experience and preferences of the attending veterinarian. A period of baseline testing (commonly 3-5 sessions) to characterize eye-specific variability precedes the planned intervention. While unilateral interventions are most common, bilateral interventions can be proposed but the IACUC will require extensive justification and absolute avoidance of bilateral blindness. Post-intervention testing occurs at a frequency governed by the sensitivity and specificity of the endpoint determination. It is common for us to perform weekly or bi-weekly post-laser testing, which requires the confirmation of onset on 2 subsequent test days (1 and 2 weeks post onset detection) (He et al., 2014b). This criterion has achieved 95% specificity among control eyes in all of our studies to date – however it means that post-mortem studies of detected “onset” occur in tissues that are at least 2 to 3 weeks past that event (0 to 30% optic nerve axon loss) (He et al., 2014b).

Pre-sacrifice testing details and the sacrifice itself are planned during the confirmation period. Sacrifice is performed under deep anesthesia, either by exsanguination alone, exsanguination in the setting of perfusion of balance salt, or exsanguination in the setting of perfusion of fixative (also referred to as perfusion fixation). The ocular tissues, brain, and other tissues of interest are then processed for storage and additional post-mortem analysis.

Acute and Chronic IOP Elevation

In both the mouse (Kong et al., 2012; Sun et al., 2013) and rat (Abbott et al., 2014; Stowell et al., 2010; Zhi et al., 2012) there is increasing use of acute (30 minute to 8 hour) manometrically controlled IOP elevation as a form of controlled challenge to the visual system. In the NHP, acute IOP elevation experiments have been performed to assess axon transport (Minckler et al., 1977; Quigley and Anderson, 1976; Quigley and Anderson, 1977a; Quigley et al., 1980) and blood flow (Hayreh et al., 1994; Liang et al., 2009; Wang et al., 2014b), but not to comparatively study ONH or retinal susceptibility. In addition they have been used to assess ONH surface (Burgoyne et al., 1995a, b; Coleman et al., 1991; Heickell et al., 2001; Strouthidis et al., 2011a) and laminar (Bellezza et al., 2003a, b; Qin et al., 2013; Strouthidis et al., 2011a; Yang et al., 2009b; Yang et al., 2011b) compliance. Experiments designed to use acute IOP elevation to characterize the molecular response of the resultant insult and recovery, to assess interventions to alter these phenomena, and to use as models of chronic IOP elevation, have not yet been attempted.

The mainstay of NHP EG research has been chronic unilateral IOP elevation through serial lasering to the trabecular meshwork of one eye. In our laboratory, after a period of baseline studies, lasering of one eye commences with a single 270 degree treatment with a Diode (previously argon) laser attached to the slit lamp in a manner similar to (but deliberately more damaging than) human argon laser trabeculoplasty (ALT) (300 mw to 1.0 mw, for 1000 msec duration, 50 to 100 micron spot size). Treatment is confluent and power is adjusted up or down to achieve dense blanching with bubbles while avoiding “pops” or bleeding. Sub-tenons dexamethasone (.5 ml or 1.0 ml of a 10 mg/ml solution) and oral meloxicam are given to reduce post-operative discomfort and photophobia which can be observed by animal care technicians as the animal’s preference for the back of the cage, (which is often less bright than the front). IOP is checked and testing is performed the following week. A second 180 degree laser treatment that includes the remaining untreated area is almost always required.

Using the above settings, it is not uncommon to require 3 to 5 lasering sessions before detected IOP becomes elevated. Because, re-treatment is common, the eye-specific clock-hours of treatment during each laser session are recorded for ongoing reference. In our hands peripheral anterior synechiae are rare and IOP elevation usually occurs in the setting of open access to the trabecular meshwork. Lasering at higher settings for longer duration increases the likelihood of achieving IOPs in the 50s and 60s. Minimal, moderate and high IOP elevations can be obtained (Gardiner et al., 2012), all of which can lead to the onset and progression of confocal scanning laser tomography (CSLT) detected ONH surface change, the timing of which being dependent upon eye-specific susceptibility. Onset less commonly occurs in the setting of no detected IOP elevation (Yang et al., 2011b). In this circumstance it is assumed that IOP is elevated during periods in which it is not being measured. Alternative explanations have previously been discussed (Yang et al., 2011b).

Our target is detected IOPs in the low to mid 20’s to most closely mimic human ocular hypertension. We have reported our strategy for characterizing the magnitude and variability of IOP insult as well as their relationship to CSLT onset and progression in a previous report (Gardiner et al., 2012). Alternative strategies of IOP elevation have been evaluated (see the

"History" section, above). A microbead model for chronic IOP elevation (Chen et al., 2010) is currently under development (personal communication, David Calkins).

IOP Measurement

For a more thorough discussion of IOP measurement in the NHP EG model, please see the companion articles by Cameron Millar (REF place holder) and Crawford Downs (REF-place holder) entitled "Non-continuous measurement of IOP in laboratory animals" and "Continuous telemetric monitoring of IOP in primate models of glaucoma", respectively. At present, we measure IOP "cage side" (immediately following ketamine administration, in the cage), and then again upon institution of isoflurane anesthesia 15 to 20 minutes later.

In Vivo Testing: Baseline and Longitudinal Follow-up

Baseline testing is done to characterize the eye-specific variability of each form of testing. The number of sessions is dependent upon the test, the presence of population-based variability estimates (Fortune et al., 2013a; Fortune et al., 2013b) (average variability based on multiple animals) and the preference for eye-specific (Fortune et al., 2013b; He et al., 2014b) versus population based (Fortune et al., 2013a; Fortune et al., 2013b) change detection. We most commonly acquire 3 to 5 baseline testing sessions. The frequency of post-laser testing is dependent upon the expected rate of change in the variable being tested, the required precision of onset detection and/or the target stage for sacrifice. We most commonly test every 1 to 2 weeks post laser.

Manometric IOP Control vs Actual IOP

The details and logic for performing both baseline and post-laser testing at manometric controlled IOP has been discussed in previous publications (Bellezza et al., 2003b; Burgoyne et al., 1995a). Weekly or bi-weekly anterior chamber manometry can induce inflammation and transient periods of hypotony post-needle removal. Iris and lens trauma can lead to anterior chamber bleeding and focal cataractous change but are rare once technicians gain experience. Our infusion fluid contains antibiotic and steroids (a standard human vitrectomy cocktail, dose-adjusted for the NHP eye) for infection and inflammation prophylaxis. In 24 years of weekly to bi-weekly testing, in more than 200 animals (in some, with up to 2.5 years of weekly tests), we have experienced a single ocular infection, which was unilateral and led to corneal opacification and loss of the animal to further testing.

Keratometry, Pachymetry, Corneal Hysteresis, Axial Length and Refraction are commonly obtained at baseline and monitored longitudinally, both to be able to most accurately employ magnification correction of retinal imaging and as an indirect measurement of ocular wall expansion and elongation through the course of chronic IOP elevation.

ONH/RNFL/Macular Structural Imaging in the NHP EG Model

See the companion article by Fortune, for details on ONH and retinal imaging in the NHP EG model. Stereoscopic optic disc and Red Free fundus photos have been employed in a series of previous publications to document the normal ONH (Quigley et al., 1991b) as well as to study ONH (Burgoyne et al., 1995c; Derick et al., 1994; Ervin et al., 2002; Varma et al., 1992) and RNFL (Jonas and Hayreh, 1999; Quigley and Addicks, 1982) change in NHP

EG. Confocal scanning laser tomography (CSLT) of the ONH (Burgoyne et al., 2002; Fortune et al., 2012; Fortune et al., 2013b), has been complimented by Scanning Laser Polarimetry (SLP) analysis of the RNFL (Fortune et al., 2013a; Fortune et al., 2012; Fortune et al., 2013b) in selective institutions. Spectral Domain Optical Coherence Tomography (SDOCT) has replaced CSLT imaging as the primary form of cross-sectional assessment and longitudinal change detection in most laboratories (He et al., 2014b; Luo et al., 2014; Patel et al., 2011; Patel et al., 2014b; Strouthidis et al., 2011a, b; Strouthidis et al., 2010; Strouthidis et al., 2009a; Strouthidis et al., 2009b; Yang et al., 2014b). See the section below on OCT phenotyping and Figures 1-5 for details. Adaptive Optics imaging of the lamina has also been implemented (Ivers et al., 2011; Sredar et al., 2013; Vilupuru et al., 2007).

Blood Flow

Laser speckle flowgraphy is currently being used to perform in vivo assessment of blood flow and autoregulation changes in the NHP eye (Cull et al., 2013; Wang et al., 2014b; Wang et al., 2012). Studies employing fluorescein angiography (Hayreh and Baines, 1972a, b), fluorescent vesicles (Khoobehi and Peyman, 1994), and laser Doppler flowmetry (Brooks et al., 2004; Petrig et al., 1999; Wang et al., 2001) precede this work.

Electrophysiology and Visual Field Testing

Electrophysiology has been performed in the NHP eye by several research groups (Cull et al., 2008; Fortune et al., 2004; Fortune et al., 2012; Fortune et al., 2015; Fortune et al., 2002; Fortune et al., 2003; Frishman et al., 2000; He et al., 2014b; Rangaswamy et al., 2006; Viswanathan et al., 1999). Humphrey static perimetry in the NHP has only been accomplished in the laboratory of Ron Harwerth (Harwerth et al., 1999; Harwerth et al., 2004; Harwerth et al., 1993; Harwerth et al., 2007; Harwerth et al., 2010).

ONH Surface Compliance Testing has been carried out in vivo using manometric IOP control and a stereoscopic video system (Burgoyne et al., 1995a, b; Burgoyne et al., 1994) followed by more extensive studies using CSLT (Heickell et al., 2001). More recently these studies have been extended to the deep ONH and peripapillary sclera using SDOCT (Qin et al., 2013; Strouthidis et al., 2011a; Yang et al., 2011a).

Axon Transport and Flow

In vivo assessment of axon transport and flow have not yet been achieved in the NHP, however a variety of tracer and viral systems (Masamizu et al., 2011) are under evaluation for intravitreal injection, retinal ganglion cell (RGC) somal penetration, and axon transport and flow evaluation.

In Vivo Orbital Optic Nerve and Brain Imaging

Positron emission tomography (PET) scanning (Imamura et al., 2009) and Magnetic Resonance Imaging (MRI) (Calkins et al., 2008) techniques are beginning to be used to study the ONH, orbital optic nerve and brain of NHPs.

Genetic Manipulation

Viral vectors (Borras et al., 2001; Charbel Issa et al., 2013; Liu et al., 1999; Vandenberghe et al., 2013), and small interfering ribonucleic acids (SiRNA) (Takahashi et al., 2014) are being developed for the NHP eye, however there has been no published implementation in the NHP EG model.

In Vitro and Ex-vivo Techniques

Cell Culture

While a variety of anterior chamber NHP cell types have been grown in cell culture, an extensive review of the literature revealed no reports of NHP optic nerve head, optic nerve or retinal astrocytes, RGCs, or scleral fibroblasts being grown in cell culture and therefore no evidence of their direct incorporation into the study of NHP EG.

Scleral, Laminar and Corneal Material Property Testing and Alteration

Young versus old normal eye (Girard et al., 2009c) and control versus EG eye (Downs et al., 2005; Girard et al., 2011) scleral material properties have been characterized using scleral shell inflation techniques in the Downs' laboratory. These studies have been extended to moderate and severe glaucoma (Downs et al., 2013) using similar experimental testing techniques, but an advanced statistical analysis.

Organ Culture

The NHP anterior chamber organ culture model has been accomplished (Hu et al., 2006), however it has not directly contributed to the NHP EG model. There is no published optic nerve head organ culture model in any species.

Post-mortem techniques

Light and Fluorescent Microscopy

There is a large literature on the light microscopic examination of the NHP retina and ONH within normal, control and EG eyes using traditional stains, immunohistochemistry and in situ hybridization (Bellezza et al., 2003b; Desatnik et al., 1996; Hayreh et al., 1999; Hayreh and Vrabec, 1966; Kalvin et al., 1966; Lampert et al., 1968; Minckler et al., 1977; Quigley and Anderson, 1976; Quigley and Anderson, 1977a; Quigley et al., 1991b; Quigley et al., 1980; Strouthidis et al., 2010; Zimmerman et al., 1967), (see reference list for additional examples). More recently, traditional collagen stains (Ponceau S and acid fuchsin) have been combined and applied to the cut surface of a paraffin-embedded ONH trephine which is then imaged with a high resolution camera after each of 800 to 1500 serial 1.5 micron sections are cut from the vitreous surface deep into the retrolaminar, orbital optic nerve (Burgoyne et al., 2004). This technique, termed 3D histomorphometric reconstruction (3D HMRN), provides a high (1.5 × 1.5 × 1.5 micron voxel) resolution digital 3D reconstruction of the ONH tissues from which digital section images can be acquired in any orientation for manual delineation (segmented) and quantification using custom software. Most recently, we have described a method for isolation of the laminar beams from 3D HMRNs and the quantification of voxel specific beam diameter, pore diameter and connective tissue volume

and volume fraction determinations (Lockwood et al., 2015). Finite element modeling techniques, (see below) have been applied to these digital geometries.

Second Harmonic and Two-photon Imaging

Ex-vivo strategies for second harmonic imaging have not been applied to the NHP eye. Ex-vivo two-photon imaging of the NHP retina has been reported (Palczewska et al., 2014).

Electron Microscopy

There is also a large literature that has utilized transmission electron microscopy (TEM) and/or scanning electron microscopy (SEM) to study the retinal, ONH and retrolaminar optic nerve tissues in normal and EG NHP eyes (Anderson, 1969a; Anderson, 1969b; Anderson, 1970; Anderson and Hoyt, 1969). Scanning block face electron microscopic (SBF-EM) 3D reconstructions of young and old control and early EG NHP ONHs are currently underway within the laboratory of Mark Ellisman (Davis et al., 2014; Nguyen et al., 2011) in a collaborative effort to extend our 3D HMRN techniques (Burgoyne et al., 2004; Lockwood et al., 2015) to nanometer resolution.

Finite Element Modeling (FEM)

For a more detailed explanation of how this engineering technique has been applied to the study of glaucoma in multiple species, see the companion article authored by Ethier and Nguyen (REF-placeholder). Within the NHP, Downs and colleagues have published a series of papers in normal, control and early EG sclera and ONH tissues (Bellezza et al., 2000; Girard et al., 2009a; Girard et al., 2009b; Girard et al., 2009c; Roberts et al., 2009; Roberts et al., 2010a; Roberts et al., 2010b).

Retinal Cell Counts

RGCs and non RGC retinal cells have been counted in normal, control and EG NHP eyes using a variety of light microscopic techniques (Cowey et al., 2011; Desatnik et al., 1996; Glovinsky et al., 1993; Harwerth et al., 1999; Levkovitch-Verbin et al., 2001; Nork et al., 2000a; Nork et al., 2000b). Their focus has been to characterize RGC subtypes, relative RGC subtype susceptibility to chronic IOP elevation, and to separately address the questions of whether non RGC retinal cells are injured in the NHP EG model and whether primary injuries to the visual cortex can cause transsynaptic degeneration of RGCs (Cowey et al., 2011).

Optic Nerve Axon Counts

A series of sub-sampling strategies for estimating the total number and size distribution of NHP orbital optic nerve axons have been summarized by Cull et al (Cull et al., 2003). We recently reported our automated method for counting 100% of the NHP optic nerve axons (Reynaud et al., 2012), and are sharing our software with all interested investigators. Our strategy for eye-specific regionalization of optic nerve axon counts relative to the foveal to Bruch's membrane opening centroid (FoBMO) axis (He et al., 2014b; Lockwood et al., 2015), so as to produce EG eye-specific FoBMO optic nerve axon loss maps that can be

compared to longitudinal SDOCT ONH, RNFL and Macular change maps, is in development.

Axon Transport

Both retrograde and anterograde tracers have been used to study axoplasmic flow and transport within the RGC axons in normal, control and NHP EG eyes (Anderson and Hendrickson, 1974; Minckler et al., 1977; Minckler et al., 1978; Minckler et al., 1976; Quigley and Anderson, 1976; Quigley et al., 1977). At present, the delivery of markers via intravitreal injection of viral vectors into NHP eyes has not been reported.

Vascular casting and microspheres

Vascular casting (Sugiyama et al., 1994), fluorescent tracers (Quigley et al., 1985), and microspheres (Alm and Bill, 1973; Geijer and Bill, 1979; Nork et al., 2006; Orgul et al., 1996a) have been used to perform post-mortem and pre-sacrifice blood flow studies of NHP eyes.

Important Concepts, Issues and Techniques

The following concepts, issues and techniques are important to the design and interpretation of NHP EG experiments, regardless of the hypotheses being tested.

The Importance of Animal-specific Hypothesis Testing

The chronic unilateral NHP EG model compares the EG eye tissues to the control eye tissues of each animal. While, there are many caveats to the following statement, serious consideration should be given during experimental design, execution and interpretation to the detection of within EG-eye change longitudinally, and EG vs. control eye differences *within each animal that is studied*. If the variability of the technique of interest will not allow within animal or within EG eye longitudinal change detection, power analyses are imperative.

Foveal-BMO Axis Colocalized Retinal/ONH/Optic Nerve Pathology

There is no anatomic justification for the standard practice of assigning “superior”, “nasal”, “temporal” and “inferior” to the ONH and retinal tissues of a given eye based on its clinical fundus photographs (Chauhan and Burgoyne, 2013; He et al., 2014b; Lockwood et al., 2015). This issue is especially important when the ability to compare equivalent regions of the NHP EG and control ONH is at the center of between-eye difference detection in NHP EG.

A large body of work (Airaksinen et al., 2008; Jansonius et al., 2009; Ogden, 1983a, b, 1984; Radius and Anderson, 1979; Stone and Johnston, 1981) supports the notion that while it is not perfect or consistent, the primate retinal nerve fiber is organized relative to the axis between the “disc” and the fovea. Since Bruch’s membrane opening (BMO) represents the actual opening through which the axons must pass, and since it can be different from the “clinical disc margin” in humans (Reis et al., 2012b) and less commonly in monkeys (Strouthidis et al., 2009b) (Figure 1A), we have begun to use the FoBMO axis (Figure 1B)

in SDOCT imaging (He et al., 2014a; He et al., 2014b) and post-mortem ONH tissues (Lockwood et al., 2015) to regionalize NHP ONH, RNFL and macular tissues. Some current OCT systems have standard software which anatomically determines the FoBMO axis at the time of initial image acquisition (Figure 2) and acquires all ONH, RNFL and macula data sets relative to it in all subsequent imaging sessions (see Phenotyping, below).

Staging

There is no agreed upon strategy for staging the NHP EG model. The current standard is to report control and EG eye optic nerve axon counts and/or Optical Coherence Tomography (OCT) RNFL thickness (RFNLT) measurements with global EG eye difference from control the outcome measure of “damage”. Within the Fortune laboratory (Fortune et al., 2013a; Fortune et al., 2015), SLP is used to detect the onset of RGC axon cytoarchitectural alteration, most commonly prior to OCT detected RNFL thickness change. Within several laboratories longitudinal electroretinography (ERG) (Cull et al., 2008; Fortune et al., 2004; Fortune et al., 2015; Fortune et al., 2002; Fortune et al., 2003; Frishman et al., 2000; He et al., 2014b; Rangaswamy et al., 2006; Viswanathan et al., 1999) testing is performed to detect the onset of functional change, and within the Harwerth laboratory visual field testing (Harwerth et al., 1999; Harwerth et al., 2004; Harwerth et al., 1993; Harwerth et al., 2007; Harwerth et al., 2010) can be performed to detect the onset and progression of visual field loss. In all instances, it is important to recognize that all current methods focus on the RGC axon and/or the RGC soma, which, while central to vision loss, may not reflect the primary pathophysiology of the larger neuropathy. As is beginning to occur for the mouse (Howell et al., 2011), and rat (Johnson et al., 2011) the NHP EG model will eventually move to more robust, cell specific, genomic (Kompass et al., 2008) and proteomic (Burgoyne et al., 2014; Crabb et al., 2014; Jang et al., 2014; Stowell et al., 2011; Stowell et al., 2014; Zhang et al., 2014) characterizations of early “glaucomatous” alteration within the ONH, retina, sclera, orbital optic nerve and lateral geniculate. As this level of knowledge grows the ‘staging” of NHP EG will likely occur within multiple tissues and pathways, be different within regions of the same ONH and retina, and be different within the “aged” compared to the “young” eye.

Phenotyping

There is also no agreed upon strategy for phenotyping the normal and glaucomatous NHP eye. However, recent advances in OCT imaging of the ONH, RNFL and macular tissues in both NHP and human eyes, should allow for more anatomically consistent quantification of these tissues in health and disease. Figures 1 – 5 illustrate our strategy for SDOCT phenotyping the ONH, RNFL and Macula of the NHP (and human) (Burgoyne, 2015) eye. In our laboratory, post-mortem 3D HMRN, immunohistochemistry, optic nerve axon counts and SBF-EM 3D reconstructions of the NHP EG eye are being colocalized to the pre-sacrifice, SDOCT EG eye change-from-baseline map (Yang et al., 2015). Other laboratories are employing NHP SDOCT phenotyping using similar strategies in their work (Patel et al., 2014a; Patel et al., 2014b).

The Contralateral *"Control"* eye may *not* be *"Normal"*

Several pieces of evidence suggest that the control eye within the NHP EG model may be altered both by the neuropathy that occurs in the contralateral EG eye and by the testing protocols that are employed to study it. It is plausible, that EG eye axon loss can affect the contralateral RGC axons within the chiasm, at the pre and post-synaptic terminals of the lateral geniculate and other RGC projection sites within the brain, or via systemic effects. Transynaptic degeneration of RGCs has been demonstrated in the NHP eye following primary unilateral removal of the visual cortex (Cowey et al., 2011). It is also possible that weekly anterior chamber cannulation (required for manometric IOP control during testing) may induce chronic, intermittent inflammation and/or hypotony (upon anterior chamber needle removal) that itself leads to ONH tissue alteration and/or RGC axon loss.

While control eye change was not prominent in our recent longitudinal SDOCT characterization of ONH and RNFLT change in early NHP EG (He et al., 2014b), two pieces of evidence in our work suggest there may be transient and/or permanent control eye alterations in NHP EG. First, we see intermittent ONH swelling by CSLT topographic change analysis (TCA) in control eyes through the course of the neuropathy. Second, the Fortune laboratory has reported control eye longitudinal loss of mfERG signal in pooled data from a total of 39 unilateral NHP EG animals (Fortune et al., 2015). Because of these concerns we are undertaking a careful comparison of control eye orbital optic nerve axon number, size and shape compared to "naive" normal eyes from bilateral-normal NHPs. The presence of control eye optic nerve axon loss or degeneration, if detected, will influence the frequency and character of our NHP EG testing protocols moving forward, and begin a search for the mechanisms whereby the EG eye pathophysiology may be altering control eye physiology.

Physiologic Inter-Eye Difference (PID) and Percent Difference (PIPD) Within Bilateral Normal Animals

When cross-sectional or post-mortem comparisons between the EG and control eye of each animal are made within the NHP EG model, we have previously discussed the need to establish PID and PIPD maxima within bilateral normal animals for all parameters of interest (Yang et al., 2009a). EG vs. control eye differences that exceed these PID and/or PIPD maximum values are more likely to represent "real" EG eye "change" rather than simply the difference between the two normal eyes of a normal animal. Eye-specific longitudinal change detection within the EG eye, as acquired through in vivo testing (He et al., 2014b), has the advantage of not requiring reference to PID or PIPD maximum values.

Important NHP Normal, Control and EG Eye Findings

This section summarizes NHP EG findings of the past 40 years that are pertinent both to our understanding NHP EG and to its implications for human glaucoma. It is by requirement brief and interested readers are directed to the primary sources.

Normal, Control and pre-EG Eye ONH Biomechanics, Blood Flow, Autoregulation and Axon Counts

The NHP ONH surface, lamina cribrosa, scleral canal and peripapillary sclera are compliant structures, demonstrating modest deformations that are reversible through the range of 0 to 45 mmHg (Bellezza et al., 2003a, b; Burgoyne et al., 1995a, b; Burgoyne et al., 1994; Coleman et al., 1991; Heickell et al., 2001; Strouthidis et al., 2011a; Yang et al., 2009b). In a given eye, CSLT- and SDOCT-detected ONH surface compliance is not representative of underlying lamina compliance (Strouthidis et al., 2011a). In subsets of eyes, scleral canal expansion and outward bowing of the peripapillary sclera are part of the ONH response. The laminar-peripapillary scleral dynamic is such that a compliant sclera exerts tensile effects on the lamina that may counter-intuitively pull it forward (i.e. inward) within the canal following acute IOP elevation (Bellezza et al., 2003a). ONH FEMs in bilateral normal animals suggest that contralateral eyes exhibit similar mechanical behavior, and that local mechanical stress and strain correlate highly with local laminar connective tissue volume fraction (a measure of connective tissue density) (Roberts et al., 2010a). In scleral material property testing using speckle interferometry which was followed by inverse FEM development, NHP sclera exhibited inhomogeneous, anisotropic, nonlinear mechanical behavior (Girard et al., 2009a; Girard et al., 2009b).

While it has been the source of substantial controversy (Hayreh, 2001), and only a few studies have been performed in NHP eyes (most having been performed in human cadaver eyes), the blood supply to the NHP ONH and retrolaminar optic nerve as determined by vascular casting (Sugiyama et al., 1994) is derived primarily from the central retinal artery for the prelaminar neural and peripapillary RNFL and from the short posterior ciliary arteries for the laminar beam and retrolaminar circulation (Hayreh, 2001; Sugiyama et al., 1994). However, the capillary beds of all three ONH regions are continuously connected (Hayreh, 2001; Sugiyama et al., 1994). Blood flow is autoregulated within the NHP ONH and retina (Alm and Bill, 1973; Liang et al., 2009; Wang et al., 2014a). Choroidal autoregulation in the NHP has not been studied. ONH autoregulation is maintained until the perfusion pressure falls below 30 mmHg (Geijer and Bill, 1979), and is diminished more by lower levels of blood pressure (BP) than by increased levels of IOP (Liang et al., 2009). Following acute IOP elevation, breakdown of the NHP ONH blood brain barrier (Radius and Anderson, 1980), and selective compromise of the immediate peripapillary choroidal circulation (Hayreh and Jonas, 2000), have been described.

Strong evidence suggests that axon transport and flow are disrupted within the lamina cribrosa in normal NHP eyes at physiologic levels of IOP (Minckler et al., 1978; Minckler and Tso, 1976). These phenomena increase following acute IOP lowering (Minckler et al., 1978; Minckler et al., 1976) and elevation (Anderson and Hendrickson, 1974; Hayreh et al., 1979; Levy, 1974; Minckler et al., 1977; Minckler et al., 1978; Minckler et al., 1976; Quigley and Anderson, 1976; Quigley and Anderson, 1977a; Quigley et al., 1980; Quigley et al., 1979).

NHP optic nerve axon counts were initially reported in a series of reports that used sub-sampling estimates (Cull et al., 2003; Morrison et al., 1990a; Ogden and Miller, 1966; Sanchez et al., 1986). Quigley reported that the size of the disc (clinically estimated within

stereophotos) and the number of optic nerve axons were linearly correlated (Quigley et al., 1991b). In a recent report using an automated method to count 100% of the axons (Reynaud et al., 2012), total optic nerve axon counts ranged from 900,000 to 1,600,000 in 46 normal and control NHP eyes.

Initial descriptions of decreased laminar beam thickness and increased laminar pore diameters within the superior and inferior scleral canal of the NHP (Radius, 1981) and human (Dandona et al., 1990; Quigley and Addicks, 1981; Radius and Gonzales, 1981) eye, were recently confirmed in 21 normal and control NHP eyes using FoBMO 3D HMRN techniques (Lockwood et al., 2015). However, in that study, eye-specific laminar microarchitectural discordance was variable among the studied eyes and connective tissue density was commonly most diminished within the inferior nasal sector.

Visual field data from normal monkeys have been shown to be comparable to those from humans with respect to: (1) sensitivity as a function of stimulus field size; (2) the derived Statpac global indices; and (3) the variance of threshold measurements across the visual field (Harwerth et al., 1993). The relationship between visual field sensitivity and RGC density for the NHP eye has been determined by test point eccentricity (Harwerth et al., 2010).

Intrinsically photosensitive RGCs have been described in the macaque retina, and their central projections and role in circadian rhythms are being clarified (Hannibal et al., 2014). Their potential contributions to NHP EG have not been studied.

Age Effects in Normal and Control Eyes

The development of the structural proteins of the neonatal and adult lamina cribrosa have been described (Morrison et al., 1989). Age-related stiffening of the NHP lamina cribrosa has been suggested by indirect (Yang et al., 2014b) and detected by direct (Qin et al., 2012) measures. Age-related stiffening of the sclera has been directly measured (Girard et al., 2009c). Age-related loss of optic nerve axons (Cull et al., 2012; Fortune et al., 2014; Morrison et al., 1990a; Sandell and Peters, 2001), RNFLT (Fortune et al., 2014), and RGC densities (Kim et al., 1996) have been characterized. However, Fortune recently detected minimal age effects within 100% optic nerve axon count data from control and normal eyes of 46 NHPs (age 1.2 – 26.7 years) (Fortune et al., 2014). Interestingly, while RNFLT declined by 4 μm per decade in that study, a rate that was three times faster than the loss of optic nerve axons, approximately one-half of this difference was explained by the combination of optical degradation leading to reduced SDOCT scan quality and thinning of the major blood vessels in the aged NHP eye. Global and FoBMO sectoral age effects on ONH Rim and RNFL in the NHP eye are currently under study to test the hypothesis that they will co-localize to the maximum sectoral effects of chronic IOP elevation (Yang et al., 2015), as has been reported in humans (Chauhan et al., 2014a; See et al., 2009).

NHP EG Eye Change

The Site of RGC Axon Transport and Flow Disruption in the Setting of Chronic IOP Elevation is Within the Lamina Cribrosa

Strong evidence suggests that axon transport disruption following chronic (Gaasterland et al., 1978; Quigley and Addicks, 1980b) IOP elevation also occurs within the lamina cribrosa of the NHP ONH. Early RGC (Weber et al., 1998) and non-RGC retinal (Nork et al., 2000b) involvement in NHP EG has been reported, however photoreceptor changes in EG have been contested (Wygnanski et al., 1995). Lateral geninculate and visual cortex changes have been described (Dandona et al., 1991; Gupta et al., 2007; Vesti et al., 2003; Yucel et al., 2000; Yucel et al., 2001), but have not been systematically looked for in brains from early EG eyes.

The Mechanisms Contributing to RGC Axon Transport Disruption and Axonal Injury Remain Unknown (Burgoyne, 2011; Morgan, 2000; Quigley, 1999)

Until proven otherwise it is reasonable to believe that the environment of the ONH represents a challenge to axonal transport and flow at statistically “normal” levels of IOP and that this challenge increases as IOP is increased and/or cerebrospinal fluid (CSF) pressure decreases (Yang et al., 2014a), through all levels of IOP and CSF pressure. While an extensive literature has attempted to establish classic “mechanical” and “vascular” components to the insult, neither can be considered unequivocally established or ruled out. Non IOP-related risk factors remain to be determined. Each, once established, may act alone or interact with IOP (Burgoyne, 2011). Their presence and magnitude of effect should be expected to enhance the susceptibility of the ONH to whatever level of IOP, CSF pressure and ocular perfusion pressure it is experiencing.

RGC Apoptosis Has Been Shown to be Present in NHP EG (Quigley et al., 1995)

Obstruction of retrograde delivery of neurotrophins (Pease et al., 2000) may be a contributing mechanism.

Connective Tissue Deformation and Remodeling Occur Early in NHP EG

Classic descriptions of glaucomatous cupping in the NHP eye by light and electron microscopy (Furuyoshi et al., 2000; Jonas et al., 2011; Lampert et al., 1968; Quigley and Addicks, 1980b) described laminar deformation, thinning, and compression accompanied by scleral canal expansion through the course of the neuropathy. Cavernous degeneration was described following very high IOP insults of short-term duration (Zimmerman et al., 1967). Pre-existing peripapillary crescents were found to become more visible through the course of NHP EG, but did not demonstrate increases in size (Derick et al., 1994).

More recently, using 3D HMRN techniques (Burgoyne et al., 2004; Yang et al., 2009a) and focusing on early EG (i.e. the onset of CSLT-detected ONH surface change − 0 to 30% optic nerve axon loss) (He et al., 2014b), posterior deformation and thickening of the lamina (Yang et al., 2007a; Yang et al., 2007b), accompanied by scleral canal expansion (Downs et al., 2007), outward bowing of the peripapillary sclera (Yang et al., 2007a; Yang et al., 2007b), and outward migration of the laminar insertion into the retrobulbar pial sheath

(Yang et al., 2011c) has been described. These phenomena, together suggested that the lamina was not just deforming in response to chronic IOP elevation but was “remodeling” itself into a new shape in response to its altered biomechanical environment (Burgoyne, 2011; Downs et al., 2011b; Hernandez, 2000; Roberts et al., 2009; Yang et al., 2011c).

One aspect of the increase in laminar thickness appears to be the addition of new beams (Roberts et al., 2009), which, combined with evidence for laminar insertion migration (Yang et al., 2011c), led Downs and colleagues to hypothesize that recruitment of the longitudinally oriented retrolaminar optic nerve septa into more transversely oriented structures may occur (Roberts et al., 2009). Interestingly, Hayreh and coworkers reported retrolaminar fibrosis in the monkey model of experimental glaucoma (Hayreh et al., 1999). This observation is compatible with retrolaminar septal recruitment, although Hayreh made no comment about the orientation of beams or their insertion into the pia, and the animals in his study were at a more advanced stage of glaucomatous damage.

Animals carried to moderate and severe axon loss demonstrate progressive laminar deformation and scleral canal expansion that, in the most severely damaged eyes, is accompanied by profound laminar thinning and pialization (Williams et al., 2013).

Indirect (Burgoyne et al., 1995a) and direct (Bellezza et al., 2003b; Girard et al., 2011; Qin et al., 2013) evidence suggest that the ONH and peripapillary scleral connective tissues become hypercompliant early in their response to chronic IOP elevation and then progress to later stiffening (Burgoyne et al., 1995a; Downs et al., 2013; Girard et al., 2011). Extracellular matrix change, as well as alterations in structural proteins such as collagen and elastin (Agapova et al., 2003; Hernandez, 2000; Hernandez et al., 2008; Morrison et al., 1990b; Quigley et al., 1994; Quigley et al., 1991a; Quigley et al., 1991c), may contribute to these phenomena.

Longitudinal SDOCT Imaging Detects Early EG Eye Laminar Deformation That Precedes Detectible RNFL Change (He et al., 2014b)

Age-related differences in the magnitude of laminar deformation were also detected (Yang et al., 2014b). The SDOCT FoBMO pattern of early EG eye ONH rim and RNFLT loss suggests that the superior, inferior and nasal sectors are most susceptible and that rim change precedes RNFLT change (Yang et al., 2015). These findings support the use of SDOCT imaging to phenotype all forms of NHP optic neuropathy (see below) and suggest that, in some instances, its use may alleviate the need to perform laborious, post-mortem studies.

Early EG Eye RGC Function and RNFL Birefringence Change Precede SDOCT-detected RNFL Thinning and Optic Nerve Axon Loss (Fortune et al., 2013a; Fortune et al., 2012; Fortune et al., 2015)

These results support the hypothesis that during the course of NHP glaucomatous neurodegeneration, axonal cytoskeletal and retinal ganglion cell functional abnormalities exist before thinning of peripapillary RNFL axon bundles begins.

Early EG Eye SDOCT-detected Laminar Deformation Precedes RNFL Retardance, RGC Functional, and RNFL Thickness Change (He et al., 2014b; Strouthidis et al., 2011b)

These data support the ONH as an early site of injury and structural alteration in NHP EG.

Age Effects in NHP EG

Three issues are currently under study in our laboratory. First, we have demonstrated that older (18.6 – 21.9 yrs) NHP eyes demonstrate less laminar deformation for a given magnitude of cumulative IOP insult than young (1.4 – 2.6 yrs) NHP eyes – when measurements are made both (longitudinally) up to and (cross-sectionally) at the onset of early EG (Yang et al., 2014b). These data indirectly suggest that there are structural stiffness differences in young and old NHP eyes that influence the 'depth" of manifest "cupping" early in NHP EG. We are separately characterizing the FoBMO pattern of SDOCT MRW (Figure 3) and RNFLT change within 8 young versus 8 old animals in a study that will be presented at the 2015 ARVO meeting (Yang et al., 2015). The purpose of this study is two-fold. First to document the FoBMO sectoral pattern of SDOCT MRW and RNFLT change in early EG to compare it to the FoBMO sectoral pattern of crossectional age effects in normal monkeys, as has been done for humans (Balwantray et al., 2015; See et al., 2009). Second, to assess the relative susceptibilities of the young and old eyes to RNFLT and orbital optic nerve axons loss, to their given cumulative IOP insults, through early onset and progression of RGC damage. The initial analyses of these data, for the first 4 young and 4 old animals, suggest that age-related differences in RGC axon susceptibility between 2 – 3 year old animals compared to 18 – 22 year old animals are not obvious (He et al., 2014b; Yang et al., 2014b). More extensive studies of "very old" NHPs (aged 28 – 40 yrs) and /or telemetric IOP insult characterization may be necessary to detect these differences in the NHP eye. Finally, studies to detect age-related differences in connective tissue remodeling (separate from axon loss) are also underway.

Memantine Has Been Shown to Protect Structure and Function in NHP EG in a Primary Study (Hare et al., 2004a; Hare et al., 2004b) and in Two Follow-up Analyses (Gabelt et al., 2012; Yucel et al., 2006)

The primary studies remain controversial, not because of the ultimate failure of the human clinical trial that followed (the results of which have never been formally published), but because, while rigorously performed using methodologies which were state of the art at the time, without telemetric IOP characterization and 100% optic nerve axon counts the clinical importance of the relatively small treatment effects were difficult to evaluate. These studies are important because they remain the only serious attempt to evaluate a clinical neuroprotective intervention in the NHP EG model. As such, they illustrate the strengths and weaknesses of the model (at the time the studies were performed) and deserve serious consideration when the next generation studies of neuroprotection are designed and executed in NHP EG.

Glutamate is Not Elevated in the Vitreous of NHP EG or ONT Eyes

After an initial positive report (Dreyer et al., 1996), two other groups found no evidence for Glutamate elevations in the vitreous of NHP EG eyes (Carter-Dawson et al., 2002; Wamsley

et al., 2005) and a third failed to find elevated vitreous Glutamate in NHP ONT eyes (Levkovitch-Verbin et al., 2001).

Regional and Axonal Sub-type EG Eye Optic Nerve Axon Loss and Susceptibility

Diffuse and focal patterns of RNFL loss has been reported in NHP EG (Jonas and Hayreh, 1999; Yang et al., 2015). Early descriptions of NHP EG eye optic nerve axon loss suggested the superior and inferior axons were most susceptible to injury from chronic IOP elevation (Quigley and Addicks, 1980b). A greater susceptibility of large versus small RGCs and RGC axons has also been suggested (Dandona et al., 1991; Desatnik et al., 1996; Glovinsky et al., 1991; Glovinsky et al., 1993; Wygnanski et al., 1995) but the interpretation of these findings have been challenged (Morgan et al., 2000). We are currently processing the control and EG eye axon counts from more than 60 NHP EG animals employing 100% axon counting techniques (Reynaud et al., 2012). While an overall superior and inferior susceptibility may emerge, preliminary analyses suggest that the EG eye-specific pattern of axon loss is quite variable. Comparisons to underlying laminar microarchitecture (Lockwood et al., 2015), prelaminar SDOCT ONH and RNFLT change (He et al., 2014b; Yang et al., 2015) and continuum FEM outputs (Roberts et al., 2009; Roberts et al., 2010a; Roberts et al., 2010b) are underway. The question of axon size-related susceptibility will also be revisited.

The Relationship Between NHP EG Eye SDOCT RNFL Loss and Optic Nerve Axon Loss is Linear But 10 to 15% Axon Loss is Present Before RNFL Loss Can Be Detected (Cull et al., 2012)

EG Eye Blood Flow and Autoregulation Change is Detectable Early in the Neuropathy

A large literature has described a variety of blood flow alterations in NHP EG (Hamasaki and Fujino, 1967; Quigley et al., 1984; Quigley et al., 1985). More recently, laser speckle flowgraphy has been used to demonstrate both blood flow and autoregulation change early in NHP EG (Cull et al., 2013; Liang et al., 2009; Wang et al., 2014b; Wang et al., 2012).

Visual Field Change

Harwerth has characterized the relationship between NHP EG eye visual field test point sensitivity loss and RGC density change by histological analysis in corresponding retinal locations (Harwerth et al., 1999; Harwerth et al., 2004; Harwerth et al., 2002). With white stimuli, the visual sensitivity losses were relatively constant (approximately 6 dB) for ganglion cell losses of less than 30% to 50%, and then with greater amounts of cell loss the visual defects were more systematically related to ganglion cell loss (approximately 0.42 dB/percent cell loss). However, because of inter-subject variability, ganglion cell losses of 40% to 50% were necessary before visual sensitivity losses exceeded NHP normal eye 95% confidence limits (Harwerth et al., 2004).

Lateral geniculate and visual cortex change has been PET scan detected in advanced NHP EG (Imamura et al., 2009)

What Defines a "*Glaucomatous*" Optic Neuropathy in the NHP Eye?

It is just as challenging to define a "glaucomatous" optic neuropathy in an NHP eye as it is in human glaucoma (Broadway et al., 1999; Burgoyne, 2015; Nicolela et al., 2001). While the classic combination of ONH "cupping" (Burgoyne, 2015) and an arcuate pattern of RGC axon bundle (Jonas and Hayreh, 1999; Yang et al., 2015) and visual field deficits (Fortune et al., 2004; Fortune et al., 2003; Gupta et al., 2007) have been demonstrated in NHP EG, have we defined these phenomena robustly enough so that emerging optic neuropathy models of non-IOP elevation (see below) can be evaluated as "glaucomatous" or "non-glaucomatous" based on current knowledge?

This question is central to the study of non-IOP-related risk factors in NHP EG and the creation of new NHP experimental models for glaucoma occurring at "normal" levels of IOP (i.e. without experimental IOP alteration of any form). Do the changes that occur when IOP is experimentally elevated have to be present in all forms of "glaucomatous" damage to the NHP visual system regardless of the level of IOP at which the neuropathy is occurring? Which aspects of the NHP EG phenotype change as the level of IOP at which EG occurs is altered? Which aspects of the NHP EG phenotype change as the susceptibility of the visual system is (potentially) altered by increasing axial length (i.e. myopia), increasing age, decreasing blood flow, diminishing autoregulation, an altered immune system, and/or changing the underlying genetics?

While more extensive in vivo and post-mortem phenotyping is required, until proven otherwise current evidence suggests that RGC axon transport obstruction within the lamina cribrosa, early ONH connective tissue deformation and remodeling, and a "sectoral", "focal" or "arcuate" (rather than diffuse) pattern of RGC axon bundle loss are together required to call an optic neuropathy "glaucomatous" in the NHP eye, regardless of the IOP at which it has occurred. However, NHP ONH biomechanics (above) suggests that the magnitude of laminar deformation and remodeling in response to a given level of IOP should be directly influenced by the magnitude of IOP, the magnitude of retrolaminar tissue pressure, the relative architectures and material properties (structural stiffness) of the lamina cribrosa and peripapillary sclera, and the "senescence" versus "reactivity" of the ONH glial cells responsible for the remodeling component of the response (Burgoyne, 2011; Ren et al., 2014; Yang et al., 2014b). It is therefore possible that in eyes without (or with mild or modest) IOP elevation, and/or stiff connective tissues, and/or senescent ONH glia and scleral fibroblasts, the connective tissue component of the neuropathy may be modest, minimal or even absent in a given eye. In this, the human phenomenon of senile sclerotic cupping (Broadway et al., 1999; Jonas and Grundler, 1996; Nicolela et al., 2001; Yang et al., 2014b) in which the magnitude of connective tissue deformation can be minimal, yet the glaucomatous pattern of visual loss remains identifiable, may be considered a precedent.

Other NHP optic neuropathy models

NHP models for unilateral anterior ischemic optic neuropathy (AION) (Chen et al., 2008; Miller et al., 2014), optic nerve transection (Burgoyne et al., 1995a; Ing et al., 2015; Levkovitch-Verbin et al., 2003; Morrison et al., 1990b; Pease et al., 2000; Quigley and Anderson, 1977b) and chronic, optic nerve endothelin exposure (Brooks et al., 2004; Cioffi and Sullivan, 1999; Cioffi et al., 2004; Orgul et al., 1996a), as well as bilateral optic neuropathy following primary CSF lowering (Yang et al., 2014a), have been described. Of these, the neuropathies in the AION and optic nerve transection models demonstrate mild (transection) to profound (AION) disc swelling followed by diffuse pallor without evident "cupping". In a longitudinal SDOCT study in 5 unilaterally transected NHPs, we will report anterior rather than posterior laminar deformation within weekly SDOCT data sets acquired through the first 60 days post-transection (Ing et al., 2015).

In the implanted endothelin pump model of unilateral optic nerve vasoconstriction, after preliminary studies in rabbits (Cioffi et al., 1995; Orgul et al., 1996b), optic nerve blood flow reduction in NHPs was characterized (Cioffi and Sullivan, 1999) and localized optic nerve axon loss in the setting of diffuse RNFL loss with shallow cupping was reported in a subset of 12 NHPs (Cioffi et al., 2004). Chauhan then reported optic nerve axon and RGC loss but infrequent (1 of 21 eyes) ONH topographic change in the rat endothelin optic neuropathy model (Chauhan et al., 2004). A follow up NHP study designed to detect longitudinal CSLT and SLP change as well as post-mortem laminar deformation within the endothelin-treated eyes of a separate group of animals failed to achieve detectable optic nerve axon loss in the endothelin eyes and its results were therefore uninterpretable (personal communication from the co-principal investigators, Jack Cioffi and Claude Burgoyne). In a later study in 5 rhesus macaques unilaterally implanted with endothelin pumps and followed for 1.5 years (Brooks et al., 2004), no significant changes in ONH morphology or ONH blood flow velocity were detected by CSLT and laser Doppler flowmetry, respectively. In that study, while optic nerve axon counts were also not significantly decreased in the endothelin treated eyes, immunohistochemical evidence of altered metabolic activity was detected in the contralateral visual cortex.

Yang and co-authors recently reported diffuse RNFL and optic nerve rim thinning in 2 of 4 NHPs following primary surgical CSF lowering (Yang et al., 2014a), A third NHP demonstrated a single nerve fiber hemorrhage, but no other change. While quantitative assessment was not reported, no qualitative evidence of laminar deformation was present within the published SDOCT images. Subsequent unpublished quantification, has confirmed that there was no SDOCT-detected laminar deformation within the four studied animals (Personal communication, Ningli Wang). While the appearance of this neuropathy is not glaucomatous by the criteria suggested above, the model is important because it demonstrates that primary CSF lowering at "normal" levels of IOP is a risk factor for RGC axon loss in a subset of NHP eyes. It therefore also suggests that in a given eye a relative increase in the translaminar pressure gradient (by whatever cause) may be a risk factor for RGC axon loss at all levels of IOP.

Targets for Model Improvement

Telemetric measurement of IOP and BP has been achieved within the Downs (Downs et al., 2011a) laboratory where there are plans to add CSF pressure in a next generation device (personal communication, Crawford Downs). Linking experimental IOP elevation and telemetric IOP monitoring to a device that pumps aqueous into the fornix, so as to both telemetrically monitor and *control* the level of IOP insult in a given eye is now required. Translation of this device to human patient care could follow for use in eyes with exceptional needs. IOP is such an important risk factor in NHP EG that to detect the presence of non IOP-related risk factors such as age, blood flow, blood flow autoregulation, immune system alteration and CSF pressure contributions to ONH and retinal susceptibility, may require certain and consistent control of the magnitude and duration of IOP insult within and between groups of animals in which other risk factors or neuroprotective interventions are varied.

In vivo MRI imaging (Calkins et al., 2008) of the laminar and retrolaminar optic nerve to seek evidence of laminar connective tissue (see above) and retrolaminar myelin remodeling (Nguyen et al., 2011; Stowell et al., 2014), early in the NHP experimental ocular hypertension are credible next steps. If confirmed using post-mortem techniques, MRI imaging could then be translated to human ocular hypertensive patient care. Enhanced in vivo imaging of laminar and peripapillary scleral architecture that includes blood flow measurements within the scleral portion of the posterior ciliary arteries, circle of Zinn-Haller, and within the laminar beam capillaries, could share the same trajectory towards human patient translation.

Polarization sensitive imaging (Baumann et al., 2012; Cense et al., 2009; Dwelle et al., 2012) of early RGC axon cytoarchitectural alterations may expand initial findings using SLP (see above). In vivo assays of axon transport as well as ONH and retinal astrocyte cellular activity may eventually reveal even earlier stages of visual system “unhappiness”. In vivo assessment of ONH, peripapillary scleral and corneal material properties will improve the accuracy of all forms of clinical FEM. Until now we have defined “early EG” in our studies as the onset of CSLT-detected ONH surface change confirmed twice (which is the most common human clinical onset criteria from structural and functional testing) and yields EG eyes with from 0 to 29% axon loss (He et al., 2014b). However, we are implementing FoBMO-sectoral, SDOCT change detection in real-time within the ONH/RNFL and macula employing trend analyses (He et al., 2014b; Yang et al., 2014b). We predict that this approach will consistently allow us to study EG eyes with less than 10% RGC axon loss.

Genomic (Howell et al., 2011; Johnson et al., 2011; Kompass et al., 2008) and proteomic (Burgoyne et al., 2014; Jang et al., 2014; Stowell et al., 2011; Stowell et al., 2014; Zhang et al., 2014) characterizations of the transition from NHP ocular hypertension to glaucomatous damage are now underway. Molecular characterization of the constituent cells of the peripapillary sclera, optic nerve head and retrolaminar optic nerve will not only enhance staging but will pave the way for viral vectors that employ cell specific promoters. In vivo detection of RGC apoptosis has been described (Cordeiro et al., 2004), but has not been incorporated into the NHP EG model. In vivo reporters for mechano-transduction, hypoxia

and oxidative stress may lead to in vivo detection of early cellular “unhappiness” that both precedes damage and is reversible. Treatments targeted to reverse such alterations may then follow.

There has been no systematic attempt to culture ONH astrocytes, RGCs or scleral fibroblasts from the NHP eye, and therefore no attempt to study or influence their cell biology at the earliest stage of NHP EG in cell culture. State of the art, 3D cell culture systems to subject ONH cells to precise levels of engineering strain without the confound of hypoxia (Lei et al., 2011) will better translate the outputs of post-mortem FEM into cellular activity. An ONH organ culture system would take advantage of the large number of post-mortem NHP eyes that can be harvested from other investigators’ non-ocular NHP experimentation. Finally, the rat and mouse genetic and experimental glaucoma models have progressed to the point that performing systematic comparative biology within and between rats (Pazos et al., 2015), mice, NHPs and humans can now be fruitful. The committed procurement of human cadaver eyes with well documented glaucoma phenotypes for such studies should therefore be encouraged.

Important Questions for NHP EG, Some of Which Require the study of Mice and Rats

The following list of questions expands upon concepts that have been discussed in a series of previous publications (Burgoyne, 2011; Burgoyne and Downs, 2008; Burgoyne et al., 2005).

1) Why do primates have a connective tissue lamina and how does this influence axonal susceptibility? Is a connective tissue lamina “protective” of the axons? Is it protective in bigger eyes or just longer living eyes, or both? If it is protective, what are the mechanisms and why are they important? Are rates of age related axon loss in mice and rats higher than in tree shrew, pig and monkey? Are there detectable differences in the susceptibility of young and old mice and rats to acute and chronic IOP elevations and is this susceptibility more than in young and old tree shrews, pigs and monkeys? The current NIH audacious goal of understanding the mechanisms of aging and disease should enhance the impact of NIH proposals to study these questions in all species.

2) If age related axon loss is not substantial within NHPs from 1 to 27 years old (Fortune et al., 2014) (see above), is it dramatically enhanced in very old animals (i.e. 28 – 40) as has been demonstrated in rats? (Cepurna et al., 2005) Do age related axon loss and glaucoma share common risk factors and demonstrate similar patterns of regional susceptibility? If we can identify the shared risk factors and manipulate them can we create an experimental model of glaucoma that does not require IOP elevation?

3) Do astrocytes have processes on the laminar capillaries in NHPs, and if they do are these processes withdrawn in early EG and with aging? Can we intervene to stabilize these processes in a beneficial way? Will such interventions, if successful, slow axon loss in both aging and EG?

4) Can a “glaucomatous” optic neuropathy be created in the NHP eye without elevating IOP? How? Will we be able to detect and defend that it is “glaucomatous”? How?

5) What are the important components of axonal nutrition within the ONH? How are these altered by age and disease? Do the laminar beam connective tissues (including the beam and basement membrane extracellular matrix (ECM)) influence nutrient diffusion and if so how? Can IOP-related stress and strain within the beams, (separate from their ECM) influence nutrient diffusion? If you make the laminar beam stiffer, is there a clinically important effect on diffusion? Are these relationships changed in age and disease?

6) Can IOP-related stress and strain within the ONH connective tissues directly diminish the volume flow of blood within the contained scleral branches of the posterior ciliary arteries and the laminar beam capillaries? (Hamasaki and Fujino, 1967; Hayreh and Jonas, 2000) What are the mechanisms of laminar beam capillary autoregulation? Are they altered in aging and do they falter early in the optic neuropathy of glaucoma?

7) Is it protective to RGC axons to make the peripapillary scleral connective tissues stiffer or more compliant? Is it protective to the astrocytes and scleral fibroblasts? To the connective tissues themselves? Does stiffening the sclera “effectively” isolate the lamina? What are the interactions between the lamina and sclera? How does altering laminar beam material properties influence astrocyte and RGC axon nutrition? How do all of these relationships change with age?

8) Is inflammation (Howell et al., 2011; Johnson et al., 2011) a component of early glaucomatous ONH injury in the NHP? (Burgoyne et al., 2014) What mechanisms? What chemokines? What stage? What treatment targets? Is the ONH blood brain barrier fragile in normal NHP eyes(Tso et al., 1975) and does it breakdown in early NHP EG? (Radius and Anderson, 1980)

9) What ONH neuroprotective target is appropriate and accessible to us right now?

10) Do astrocytes proliferate early in the neuropathy of NHP EG?

11) Do astrocytes migrate away from the beams early in the optic neuropathy of NHP EG? If this is true, are the cells that migrate new cells (the result of astrocyte proliferation) - leaving laminar beam astrocytes and their processes in place - or are these the cells that were previously anchored to the beam and have truly migrated away from it?

12) Do astrocytes phagocytose myelin and axonal mitochondria as part of the support they provide to the RGC axon within and behind the lamina? (Davis et al., 2014; Nguyen et al., 2011) Do they abandon this role when they migrate and or proliferate, if they do? Do they abandon this role in early NHP EG?

13) How many different cell types are there in the ONH and do they have functional roles that separately contribute to the optic neuropathy of glaucoma? ONH lamina cribrosa cells have been described in humans (Hernandez et al., 1988) but there is no description of this cell type in the NHP. What are the relationships between peripapillary scleral fibroblasts, laminar insertion site astrocytes, lamina cribrosa cells and laminar beam astrocytes? Microglia? Oligodendrocytes? Do monocytes (Howell et al., 2011; Howell et al., 2013; Howell et al., 2012) enter the ONH parenchyma in early NHP EG?

14) What is the mechanism of RGC axonal injury within the lamina? Is stabilizing RGC axon function through the lamina all we need to do? Are their larger drivers of ONH physiology that govern this task? What are they? Are they active at all levels of aging, IOP and stage of damage?

15) How many stages of molecular alteration precede detectable structural damage in the ONH and retina? (Howell et al., 2011) In what cells do they occur earliest? At what point are they irreversible? At what point do they cause damage? Damage to what structure, function and cell? Are their targets for neuroprotection in these answers?

16) Is the NHP EG model robust enough, to accurately predict neuroprotective efficacy in human glaucoma? First, is the model robust enough to detect efficacy when it is present in the NHP eye? Second, will efficacy in the NHP eye translate to human glaucoma patients? Regarding the model, if bilateral IOP, as well as BP and (perhaps) CSF monitoring are achieved, bilateral IOP control is achieved, bilateral IOP elevation in elderly animals is allowed, (likely if studies are carried to pre-perimetric levels of damage), the neuroprotective intervention is unilateral and the study utilizes FoBMO longitudinal SDOCT and 100% post-mortem optic nerve axon counts to assess the delay or reduction of RGC axon loss in the setting of chronic, modest IOP elevation - the model will likely detect clinically significant efficacy using 8-12 animals (and proper controls). Regarding the question of whether NHP efficacy will translate to humans – lessons learned from the Memantine study (above) and the United Kingdom Glaucoma Treatment Study (Garway-Heath et al., 2014) will need to be implemented in the human trial.

Acknowledgments

It is not possible to cite all authors who have made important contributions to the execution and characterization of the NHP EG model. For those I have missed due to negligence, I sincerely apologize. I have been fortunate to be NIH funded to study aging and EG in the NHP eye for 18 years. With that come biases which have influenced the organization and execution of this summary. I am a consultant to and receive unrestricted research support from Heidelberg Engineering to translate my laboratory's NHP findings to human glaucoma patient imaging. Significant portions of our SDOCT based concepts and discoveries in NHPs have been incorporated into Heidelberg's SDOCT strategies for imaging the ONH, RNFL and macula in humans. I receive occasional travel support but hold no intellectual property and receive no honorarium or personal income from this collaboration.

Supported in part by NIH grants R01EY011610 (CFB) and R01EY021281 (CFB) from the National Eye Institute, National Institutes of Health, Bethesda, Maryland; The Legacy Good Samaritan Foundation, Portland, Oregon; the Sears Trust for Biomedical Research, Mexico, Missouri; the Alcon Research Institute, Fort Worth, Texas; and an unrestricted grant from Heidelberg Engineering.

REFERENCES

Abbott CJ, et al. Evaluation of retinal nerve fiber layer thickness and axonal transport 1 and 2 weeks after 8 hours of acute intraocular pressure elevation in rats. Invest Ophthalmol Vis Sci. 2014; 55:674–687. [PubMed: 24398096]

Agapova OA, et al. Differential expression of matrix metalloproteinases in monkey eyes with experimental glaucoma or optic nerve transection. Brain Res. 2003; 967:132–143. [PubMed: 12650974]

Airaksinen PJ, et al. Conformal geometry of the retinal nerve fiber layer. Proc Natl Acad Sci USA. 2008; 105:19690–19695. [PubMed: 19066221]

Alm A, Bill A. Ocular and optic nerve blood flow at normal and increased intraocular pressures in monkeys (Macaca irus): a study with radioactively labelled microspheres including flow determinations in brain and some other tissues. Exp Eye Res. 1973; 15:15–29. [PubMed: 4630581]

Anderson DR. Ultrastructure of human and monkey lamina cribrosa and optic nerve head. Arch Ophthalmol. 1969a; 82:800–814. [PubMed: 4982225]

Anderson DR. Ultrastructure of Meningeal Sheaths: Normal Human and Monkey Optic Nerves. Arch Ophthalmol. 1969b; 82:659–674. [PubMed: 4981605]

Anderson DR. Ultrastructure of the optic nerve head. Arch Ophthalmol. 1970; 83:63–73. [PubMed: 4983627]

Anderson DR, Hendrickson A. Effect of intraocular pressure on rapid axoplasmic transport in monkey optic nerve. Invest Ophthalmol. 1974; 13:771–783. [PubMed: 4137635]

Anderson DR, Hoyt WF. Ultrastructure of intraorbital portion of human and monkey optic nerve. Arch Ophthalmol. 1969; 82:506–530. [PubMed: 4981187]

Balwantray CC, et al. Bruch's Membrane Opening-Minimum Rim Width and Retinal Nerve Fibre Layer Thickness in a Normal White Population. A Multi-centre Study. Ophthalmology. 2015 Accepted for Publication.

Baumann B, et al. Swept source/Fourier domain polarization sensitive optical coherence tomography with a passive polarization delay unit. Opt Express. 2012; 20:10229–10241. [PubMed: 22535114]

Bellezza AJ, et al. The optic nerve head as a biomechanical structure: initial finite element modeling. Invest Ophthalmol Vis Sci. 2000; 41:2991–3000. [PubMed: 10967056]

Bellezza AJ, et al. Anterior scleral canal geometry in pressurised (IOP 10) and non-pressurised (IOP 0) normal monkey eyes. Br J Ophthalmol. 2003a; 87:1284–1290. [PubMed: 14507767]

Bellezza AJ, et al. Deformation of the lamina cribrosa and anterior scleral canal wall in early experimental glaucoma. Invest Ophthalmol Vis Sci. 2003b; 44:623–637. [PubMed: 12556392]

Borras T, et al. Non-invasive observation of repeated adenoviral GFP gene delivery to the anterior segment of the monkey eye in vivo. J Gene Med. 2001; 3:437–449. [PubMed: 11601757]

Broadway DC, et al. Optic disk appearances in primary open-angle glaucoma. Surv Ophthalmol. 1999; 43(Suppl 1):S223–243. [PubMed: 10416767]

Brooks DE, et al. Functional and structural analysis of the visual system in the rhesus monkey model of optic nerve head ischemia. Invest Ophthalmol Vis Sci. 2004; 45:1830–1840. [PubMed: 15161847]

Burgoyne CF. A biomechanical paradigm for axonal insult within the optic nerve head in aging and glaucoma. Exp Eye Res. 2011; 93:120–132. [PubMed: 20849846]

Burgoyne CF. The morphological difference between glaucoma and other optic neuropathies. J Neuroophthalmol. 2015 Accepted for publication.

Burgoyne CF, Downs JC. Premise and prediction-how optic nerve head biomechanics underlies the susceptibility and clinical behavior of the aged optic nerve head. J Glaucoma. 2008; 17:318–328. [PubMed: 18552618]

Burgoyne CF, et al. Three-dimensional reconstruction of normal and early glaucoma monkey optic nerve head connective tissues. Invest Ophthalmol Vis Sci. 2004; 45:4388–4399. [PubMed: 15557447]

Burgoyne CF, et al. The optic nerve head as a biomechanical structure: a new paradigm for understanding the role of IOP-related stress and strain in the pathophysiology of glaucomatous optic nerve head damage. Prog Retin Eye Res. 2005; 24:39–73. [PubMed: 15555526]

Burgoyne CF, et al. Change detection in regional and volumetric disc parameters using longitudinal confocal scanning laser tomography. Ophthalmology. 2002; 109:455–466. [PubMed: 11874746]

Burgoyne CF, et al. Early changes in optic disc compliance and surface position in experimental glaucoma. Ophthalmology. 1995a; 102:1800–1809. [PubMed: 9098280]

Burgoyne CF, et al. Measurement of optic disc compliance by digitized image analysis in the normal monkey eye. Ophthalmology. 1995b; 102:1790–1799. [PubMed: 9098279]

Burgoyne CF, et al. Comparison of clinician judgment with digitized image analysis in the detection of induced optic disk change in monkey eyes. Am J Ophthalmol. 1995c; 120:176–183. [PubMed: 7639301]

Burgoyne CF, et al. Non-Human Primate (NHP) Optic Nerve Head (ONH) Proteomic Change In Early Experimental Glaucoma (EEG). 2014 ARVO Meeting Abstracts. 55, ARVO Abstract# 4555.

Burgoyne CF, et al. Global and regional detection of induced optic disc change by digitized image analysis. Arch Ophthalmol. 1994; 112:261–268. [PubMed: 8311780]

Calkins DJ, et al. Manganese-enhanced MRI of the DBA/2J mouse model of hereditary glaucoma. Invest Ophthalmol Vis Sci. 2008; 49:5083–5088. [PubMed: 18552381]

Carter-Dawson L, et al. Vitreal glutamate concentration in monkeys with experimental glaucoma. Invest Ophthalmol Vis Sci. 2002; 43:2633–2637. [PubMed: 12147596]

Cense B, et al. Retinal imaging with polarization-sensitive optical coherence tomography and adaptive optics. Opt. Express. 2009; 17:21634–21651. [PubMed: 19997405]

Cepurna WO, et al. Age related optic nerve axonal loss in adult Brown Norway rats. Exp Eye Res. 2005; 80:877–884. [PubMed: 15939045]

Charbel Issa P, et al. Assessment of tropism and effectiveness of new primate-derived hybrid recombinant AAV serotypes in the mouse and primate retina. PLoS One. 2013; 8:e60361. [PubMed: 23593201]

Chauhan BC, Burgoyne CF. From clinical examination of the optic disc to clinical assessment of the optic nerve head: a paradigm change. Am J Ophthalmol. 2013; 156:218–227. e212. [PubMed: 23768651]

Chauhan BC, et al. Characteristics of an Anatomically and Geometrically Accurate Neuroretinal Rim Parameter in a Normal Population. A Multi-Centre Study. 2014a ARVO Meeting Abstracts. 55, ARVO Abstract# 4028.

Chauhan BC, et al. Model of endothelin-1-induced chronic optic neuropathy in rat. Invest Ophthalmol Vis Sci. 2004; 45:144–152. [PubMed: 14691166]

Chauhan BC, et al. Enhanced detection of open-angle glaucoma with an anatomically accurate optical coherence tomography-derived neuroretinal rim parameter. Ophthalmology. 2013; 120:535–543. [PubMed: 23265804]

Chauhan BC, et al. Imaging of the temporal raphe with optical coherence tomography. Ophthalmology. 2014b; 121:2287–2288. [PubMed: 25156139]

Chen CS, et al. A primate model of nonarteritic anterior ischemic optic neuropathy. Invest Ophthalmol Vis Sci. 2008; 49:2985–2992. [PubMed: 18326695]

Chen H, et al. Optic Neuropathy Due to Microbead-Induced Elevated Intraocular Pressure in the Mouse. Invest. Ophthalmol. Vis. Sci. 2010 iovs.09-5115.

Chen TC. Spectral domain optical coherence tomography in glaucoma: qualitative and quantitative analysis of the optic nerve head and retinal nerve fiber layer (an AOS thesis). Trans Am Ophthalmol Soc. 2009; 107:254–281. [PubMed: 20126502]

Cioffi GA, et al. An in vivo model of chronic optic nerve ischemia: the dose-dependent effects of endothelin-1 on the optic nerve microvasculature. Curr Eye Res. 1995; 14:1147–1153. [PubMed: 8974844]

Cioffi GA, Sullivan P. The effect of chronic ischemia on the primate optic nerve. Eur J Ophthalmol. 1999; 9(Suppl 1):S34–36. [PubMed: 10230604]

Cioffi GA, et al. Chronic ischemia induces regional axonal damage in experimental primate optic neuropathy. Arch Ophthalmol. 2004; 122:1517–1525. [PubMed: 15477464]

Coleman AL, et al. Displacement of the optic nerve head by acute changes in intraocular pressure in monkey eyes. Ophthalmology. 1991; 98:35–40. [PubMed: 2023730]

Cordeiro MF, et al. Real-time imaging of single nerve cell apoptosis in retinal neurodegeneration. Proc Natl Acad Sci U S A. 2004; 101:13352–13356. [PubMed: 15340151]

Cowey A, et al. Transneuronal retrograde degeneration of retinal ganglion cells and optic tract in hemianopic monkeys and humans. Brain. 2011; 134:2149–2157. [PubMed: 21705429]

Crabb JS, et al. Quantitative Proteomic Analysis of Non-Human Primate (NHP) Peripapillary (PP) Sclera in Early Experimental Glaucoma (EEG). 2014 ARVO Meeting Abstracts. 55, ARVO Abstract# 5704.

Cull G, et al. Longitudinal hemodynamic changes within the optic nerve head in experimental glaucoma. Invest Ophthalmol Vis Sci. 2013; 54:4271–4277. [PubMed: 23737471]

Cull G, et al. Estimating normal optic nerve axon numbers in non-human primate eyes. J Glaucoma. 2003; 12:301–306. [PubMed: 12897574]

Cull GA, et al. Changes in Retinal Function After Onset of Experimental Glaucoma or Optic Nerve Transection in Non-Human Primates. Invest Ophthalmol Vis Sci. 2008 49, ARVO Abstract# 717.

Cull GA, et al. Relationship between orbital optic nerve axon counts and retinal nerve fiber layer thickness measured by spectral domain optical coherence tomography. Invest Ophthalmol Vis Sci. 2012; 53:7766–7773. [PubMed: 23125332]

Dandona L, et al. Selective effects of experimental glaucoma on axonal transport by retinal ganglion cells to the dorsal lateral geniculate nucleus. Invest Ophthalmol Vis Sci. 1991; 32:1593–1599. [PubMed: 1707861]

Dandona L, et al. Quantitative regional structure of the normal human lamina cribrosa. A racial comparison. Arch Ophthalmol. 1990; 108:393–398. [PubMed: 2310342]

Davis CH, et al. Transcellular degradation of axonal mitochondria. Proc Natl Acad Sci U S A. 2014; 111:9633–9638. [PubMed: 24979790]

Dawson WW, et al. Signs of glaucoma in rhesus monkeys from a restricted gene pool. J Glaucoma. 1998; 7:343–348. [PubMed: 9786564]

Dawson WW, et al. Primary open angle glaucomas in the rhesus monkey. Br J Ophthalmol. 1993; 77:302–310. [PubMed: 8318468]

Dawson WW, et al. Repeat sample intraocular pressure variance in induced and naturally ocular hypertensive monkeys. J Glaucoma. 2005; 14:426–431. [PubMed: 16276272]

Derick RJ, et al. A clinical study of peripapillary crescents of the optic disc in chronic experimental glaucoma in monkey eyes. Arch Ophthalmol. 1994; 112:846–850. [PubMed: 8002845]

Desatnik H, et al. Study of central retinal ganglion cell loss in experimental glaucoma in monkey eyes. J Glaucoma. 1996; 5:46–53. [PubMed: 8795733]

Downs JC. Optic nerve head biomechanics in aging and disease. Exp Eye Res. 2015; 133:19–29. [PubMed: 25819451]

Downs JC, et al. 24-hour IOP telemetry in the nonhuman primate: implant system performance and initial characterization of IOP at multiple timescales. Invest Ophthalmol Vis Sci. 2011a; 52:7365–7375. [PubMed: 21791586]

Downs JC, et al. IOP Exposure Determines Scleral Shell Strain Changes in Nonhuman Primate (NHP) Experimental Glaucoma. 2013

Downs JC, et al. Glaucomatous cupping of the lamina cribrosa: a review of the evidence for active progressive remodeling as a mechanism. Exp Eye Res. 2011b; 93:133–140. [PubMed: 20708001]

Downs JC, et al. Viscoelastic material properties of the peripapillary sclera in normal and early-glaucoma monkey eyes. Invest Ophthalmol Vis Sci. 2005; 46:540–546. [PubMed: 15671280]

Downs JC, et al. Three-dimensional histomorphometry of the normal and early glaucomatous monkey optic nerve head: neural canal and subarachnoid space architecture. Invest Ophthalmol Vis Sci. 2007; 48:3195–3208. [PubMed: 17591889]

Dreyer EB, et al. Elevated glutamate levels in the vitreous body of humans and monkeys with glaucoma. Arch Ophthalmol. 1996; 114:299–305. [PubMed: 8600890]

Dwelle J, et al. Thickness, phase retardation, birefringence, and reflectance of the retinal nerve fiber layer in normal and glaucomatous non-human primates. Invest Ophthalmol Vis Sci. 2012; 53:4380–4395. [PubMed: 22570345]

Ervin JC, et al. Clinician change detection viewing longitudinal stereophotographs compared to confocal scanning laser tomography in the LSU Experimental Glaucoma (LEG) Study. Ophthalmology. 2002; 109:467–481. [PubMed: 11874747]

Fortune B, et al. Inter-ocular and inter-session reliability of the electroretinogram photopic negative response (PhNR) in non-human primates. Exp Eye Res. 2004; 78:83–93. [PubMed: 14667830]

Fortune B, et al. Onset and progression of peripapillary retinal nerve fiber layer (RNFL) retardance changes occur earlier than RNFL thickness changes in experimental glaucoma. Invest Ophthalmol Vis Sci. 2013a; 54:5653–5661. [PubMed: 23847322]

Fortune B, et al. Structural and functional abnormalities of retinal ganglion cells measured in vivo at the onset of optic nerve head surface change in experimental glaucoma. Invest Ophthalmol Vis Sci. 2012; 53:3939–3950. [PubMed: 22589428]

Fortune B, et al. Relating retinal ganglion cell function and retinal nerve fiber layer (RNFL) retardance to progressive loss of RNFL thickness and optic nerve axons in experimental glaucoma. Invest Ophthalmol Vis Sci. 2015 Submitted for Publication.

Fortune B, et al. Factors affecting the use of multifocal electroretinography to monitor function in a primate model of glaucoma. Doc Ophthalmol. 2002; 105:151–178. [PubMed: 12462442]

Fortune B, et al. The Effect of Age on Optic Nerve Axon Counts, SDOCT Scan Quality, and Peripapillary Retinal Nerve Fiber Layer Thickness Measurements in Rhesus Monkeys. Transl Vis Sci Technol. 2014; 3:2. [PubMed: 24932430]

Fortune B, et al. Does optic nerve head surface topography change prior to loss of retinal nerve fiber layer thickness: a test of the site of injury hypothesis in experimental glaucoma. PLoS One. 2013b; 8:e77831. [PubMed: 24204989]

Fortune B, et al. Idiopathic bilateral optic atrophy in the rhesus macaque. Invest Ophthalmol Vis Sci. 2005; 46:3943–3956. [PubMed: 16249467]

Fortune B, et al. Local ganglion cell contributions to the macaque electroretinogram revealed by experimental nerve fiber layer bundle defect. Invest Ophthalmol Vis Sci. 2003; 44:4567–4579. [PubMed: 14507906]

Frishman LJ, et al. Effects of experimental glaucoma in macaques on the multifocal ERG. Multifocal ERG in laser-induced glaucoma. Doc Ophthalmol. 2000; 100:231–251. [PubMed: 11142748]

Furuyoshi N, et al. Vascular and glial changes in the retrolaminar optic nerve in glaucomatous monkey eyes. Ophthalmologica. 2000; 214:24–32. [PubMed: 10657742]

Gaasterland D, Kupfer C. Experimental glaucoma in the rhesus monkey. Invest Ophthalmol. 1974; 13:455–457. [PubMed: 4208801]

Gaasterland D, et al. Axoplasmic flow during chronic experimental glaucoma. 1. Light and electron microscopic studies of the monkey optic nervehead during development of glaucomatous cupping. Invest Ophthalmol Vis Sci. 1978; 17:838–846. [PubMed: 81192]

Gabelt BT, et al. Structure/function studies and the effects of memantine in monkeys with experimental glaucoma. Invest Ophthalmol Vis Sci. 2012; 53:2368–2376. [PubMed: 22427549]

Gardiner SK, et al. Intraocular pressure magnitude and variability as predictors of rates of structural change in non-human primate experimental glaucoma. Exp Eye Res. 2012; 103:1–8. [PubMed: 22960316]

Gardiner SK, et al. A method to estimate the amount of neuroretinal rim tissue in glaucoma: comparison with current methods for measuring rim area. Am J Ophthalmol. 2014; 157:540–549. e541-542. [PubMed: 24239775]

Garway-Heath DF, et al. Latanoprost for open-angle glaucoma (UKGTS): a randomised, multicentre, placebo-controlled trial. Lancet. 2014

Geijer C, Bill A. Effects of raised intraocular pressure on retinal, prelaminar, laminar, and retrolaminar optic nerve blood flow in monkeys. Invest Ophthalmol Vis Sci. 1979; 18:1030–1042. [PubMed: 90027]

Girard MJ, et al. Peripapillary and posterior scleral mechanics--part II: experimental and inverse finite element characterization. J Biomech Eng. 2009a; 131:051012. [PubMed: 19388782]

Girard MJ, et al. Peripapillary and posterior scleral mechanics--part I: development of an anisotropic hyperelastic constitutive model. J Biomech Eng. 2009b; 131:051011. [PubMed: 19388781]

Girard MJ, et al. Scleral biomechanics in the aging monkey eye. Invest Ophthalmol Vis Sci. 2009c; 50:5226–5237. [PubMed: 19494203]

Girard MJ, et al. Biomechanical changes in the sclera of monkey eyes exposed to chronic IOP elevations. Invest Ophthalmol Vis Sci. 2011; 52:5656–5669. [PubMed: 21519033]

Glovinsky Y, et al. Retinal ganglion cell loss is size dependent in experimental glaucoma. Invest Ophthalmol Vis Sci. 1991; 32:484–491. [PubMed: 2001923]

Glovinsky Y, et al. Foveal ganglion cell loss is size dependent in experimental glaucoma. Invest Ophthalmol Vis Sci. 1993; 34:395–400. [PubMed: 8440594]

Gupta N, et al. Chronic ocular hypertension induces dendrite pathology in the lateral geniculate nucleus of the brain. Exp Eye Res. 2007; 84:176–184. [PubMed: 17094963]

Hamasaki DI, Ellerman N. Abolition of the Electroretinogram Following Injection of Alpha-Chymotrypsin into the Vitreous and Anterior Chamber of Monkey. Arch Ophthalmol. 1965; 73:843–850. [PubMed: 14302520]

Hamasaki DI, Fujino T. Effect of intraocular pressure on ocular vessels. Filling with India ink. Arch Ophthalmol. 1967; 78:369–379. [PubMed: 4962803]

Hannibal J, et al. Central projections of intrinsically photosensitive retinal ganglion cells in the macaque monkey. J Comp Neurol. 2014; 522:2231–2248. [PubMed: 24752373]

Hare WA, et al. Efficacy and safety of memantine treatment for reduction of changes associated with experimental glaucoma in monkey, I: Functional measures. Invest Ophthalmol Vis Sci. 2004a; 45:2625–2639. [PubMed: 15277486]

Hare WA, et al. Efficacy and safety of memantine treatment for reduction of changes associated with experimental glaucoma in monkey, II: Structural measures. Invest. Ophthalmol. Vis. Sci. 2004b; 45:2640–2651. [PubMed: 15277487]

Harwerth RS, et al. Ganglion cell losses underlying visual field defects from experimental glaucoma. Invest Ophthalmol Vis Sci. 1999; 40:2242–2250. [PubMed: 10476789]

Harwerth RS, et al. Neural losses correlated with visual losses in clinical perimetry. Invest. Ophthalmol. Vis. Sci. 2004; 45:3152–3160. [PubMed: 15326134]

Harwerth RS, et al. Visual field defects and neural losses from experimental glaucoma. Prog Retin Eye Res. 2002; 21:91–125. [PubMed: 11906813]

Harwerth RS, et al. Behavioral perimetry in monkeys. Invest Ophthalmol Vis Sci. 1993; 34:31–40. [PubMed: 8425837]

Harwerth RS, et al. The Relationship between Nerve Fiber Layer and Perimetry Measurements. Invest. Ophthalmol. Vis. Sci. 2007; 48:763–773. [PubMed: 17251476]

Harwerth RS, et al. Linking structure and function in glaucoma. Prog Retin Eye Res. 2010; 29:249–271. [PubMed: 20226873]

Hayreh SS. The blood supply of the optic nerve head and the evaluation of it -myth and reality. Prog Retin Eye Res. 2001; 20:563–593. [PubMed: 11470451]

Hayreh SS, Baines JA. Occlusion of the posterior ciliary artery. 3. Effects on the optic nerve head. Br J Ophthalmol. 1972a; 56:754–764. [PubMed: 4213273]

Hayreh SS, Baines JA. Occlusion of the posterior ciliary artery. I. Effects on choroidal circulation. Br J Ophthalmol. 1972b; 56:719–735. [PubMed: 4213272]

Hayreh SS, et al. Effects of high intraocular pressure on the glucose metabolism in the retina and optic nerve in old atherosclerotic monkeys. Graefes Arch Clin Exp Ophthalmol. 1994; 232:745–752. [PubMed: 7890189]

Hayreh SS, Jonas JB. Optic disk and retinal nerve fiber layer damage after transient central retinal artery occlusion: an experimental study in rhesus monkeys. Am J Ophthalmol. 2000; 129:786–795. [PubMed: 10926989]

Hayreh SS, et al. Pathogenesis of block of rapid orthograde axonal transport by elevated intraocular pressure. Exp Eye Res. 1979; 28:515–523. [PubMed: 87337]

Hayreh SS, et al. Morphologic changes in chronic high-pressure experimental glaucoma in rhesus monkeys. J Glaucoma. 1999; 8:56–71. [PubMed: 10084276]

Hayreh SS, Vrabec F. The structure of the head of the optic nerve in rhesus monkey. Am J Ophthalmol. 1966; 61:136–150. [PubMed: 4159427]

He L, et al. Anatomic vs. acquired image frame discordance in spectral domain optical coherence tomography minimum rim measurements. PLoS One. 2014a; 9:e92225. [PubMed: 24643069]

He L, et al. Longitudinal detection of optic nerve head changes by spectral domain optical coherence tomography in early experimental glaucoma. Invest Ophthalmol Vis Sci. 2014b; 55:574–586. [PubMed: 24255047]

Heickell AG, et al. Optic disc surface compliance testing using confocal scanning laser tomography in the normal monkey eye. J Glaucoma. 2001; 10:369–382. [PubMed: 11711833]

Helb HM, et al. Clinical evaluation of simultaneous confocal scanning laser ophthalmoscopy imaging combined with high-resolution, spectral-domain optical coherence tomography. Acta Ophthalmol. 2010; 88:842–849. [PubMed: 19706019]

Hernandez MR. The optic nerve head in glaucoma: role of astrocytes in tissue remodeling. Prog Retin Eye Res. 2000; 19:297–321. [PubMed: 10749379]

Hernandez MR, et al. Cell culture of the human lamina cribrosa. Invest Ophthalmol Vis Sci. 1988; 29:78–89. [PubMed: 3275593]

Hernandez MR, et al. Astrocytes in glaucomatous optic neuropathy. Prog Brain Res. 2008; 173:353–373. [PubMed: 18929121]

Hosseini H, et al. Measurement of the optic disc vertical tilt angle with spectral-domain optical coherence tomography and influencing factors. Am J Ophthalmol. 2013; 156:737–744. [PubMed: 23891337]

Howell GR, et al. Molecular clustering identifies complement and endothelin induction as early events in a mouse model of glaucoma. J Clin Invest. 2011

Howell GR, et al. Deficiency of complement component 5 ameliorates glaucoma in DBA/2J mice. J Neuroinflammation. 2013; 10:76. [PubMed: 23806181]

Howell GR, et al. Radiation treatment inhibits monocyte entry into the optic nerve head and prevents neuronal damage in a mouse model of glaucoma. J Clin Invest. 2012; 122:1246–1261. [PubMed: 22426214]

Hu Y, et al. Monkey organ-cultured anterior segments: technique and response to H-7. Exp Eye Res. 2006; 82:1100–1108. [PubMed: 16442525]

Imamura K, et al. Molecular imaging reveals unique degenerative changes in experimental glaucoma. Neuroreport. 2009; 20:139–144. [PubMed: 19057418]

Ing E, et al. Lamina Cribrosa Position in the Non-Human Primate (NHP) Optic Nerve Transection (ONT) Model of a NonGlaucomatous Optic Neuropathy. 2015 ARVO Abstract# Manuscript in Preparation.

Ivers KM, et al. Reproducibility of measuring lamina cribrosa pore geometry in human and nonhuman primates with in vivo adaptive optics imaging. Invest Ophthalmol Vis Sci. 2011; 52:5473–5480. [PubMed: 21546533]

Jang G-F, et al. Quantitative Proteomic Analysis Of Non-Human Primate (NHP) Retina In Early Experimental Glaucoma (EEG). 2014 ARVO Meeting Abstracts. 55, ARVO Abstract# 4524.

Jansonius NM, et al. A mathematical description of nerve fiber bundle trajectories and their variability in the human retina. Vision Res. 2009; 49:2157–2163. [PubMed: 19539641]

Johnson EC, et al. Cell proliferation and interleukin-6-type cytokine signaling are implicated by gene expression responses in early optic nerve head injury in rat glaucoma. Invest Ophthalmol Vis Sci. 2011; 52:504–518. [PubMed: 20847120]

Jonas JB, Grundler A. Optic disc morphology in "age-related atrophic glaucoma". Graefes Arch Clin Exp Ophthalmol. 1996; 234:744–749. [PubMed: 8986446]

Jonas JB, Hayreh SS. Localised retinal nerve fibre layer defects in chronic experimental high pressure glaucoma in rhesus monkeys. Br J Ophthalmol. 1999; 83:1291–1295. [PubMed: 10535860]

Jonas JB, et al. Thickness of the lamina cribrosa and peripapillary sclera in Rhesus monkeys with nonglaucomatous or glaucomatous optic neuropathy. Acta Ophthalmol. 2011; 89:e423–427. [PubMed: 21332675]

Kalvin NH, et al. Experimental glaucoma in monkeys. I. Relationship between intraocular pressure and cupping of the optic disc and cavernous atrophy of the optic nerve. Arch Ophthalmol. 1966; 76:82–93. [PubMed: 4957379]

Khoobehi B, Peyman GA. Fluorescent vesicle system. A new technique for measuring blood flow in the retina. Ophthalmology. 1994; 101:1716–1726. [PubMed: 7936571]

Kim CB, et al. Effects of aging on the densities, numbers, and sizes of retinal ganglion cells in rhesus monkey. Neurobiol Aging. 1996; 17:431–438. [PubMed: 8725905]

Komaromy AM, et al. Diurnal intraocular pressure curves in healthy rhesus macaques (Macaca mulatta) and rhesus macaques with normotensive and hypertensive primary open-angle glaucoma. J Glaucoma. 1998; 7:128–131. [PubMed: 9559500]

Kompass KS, et al. Bioinformatic and statistical analysis of the optic nerve head in a primate model of ocular hypertension. BMC Neurosci. 2008; 9:93. [PubMed: 18822132]

Kong YX, et al. Impact of aging and diet restriction on retinal function during and after acute intraocular pressure injury. Neurobiol Aging. 2012; 33(1126):e1115–1125.

Lamparter J, et al. The influence of intersubject variability in ocular anatomical variables on the mapping of retinal locations to the retinal nerve fiber layer and optic nerve head. Invest Ophthalmol Vis Sci. 2013; 54:6074–6082. [PubMed: 23882689]

Lampert PW, et al. Pathology of the optic nerve in experimental acute glaucoma. Electron microscopic studies. Invest. Ophthalmol. Vis. Sci. 1968; 7:199–213.

Lei Y, et al. In vitro models for glaucoma research: effects of hydrostatic pressure. Invest Ophthalmol Vis Sci. 2011; 52:6329–6339. [PubMed: 21693606]

Lessell S, Kuwabara T. Experimental alpha-chymotrypsin glaucoma. Arch Ophthalmol. 1969; 81:853–864. [PubMed: 4977440]

Levkovitch-Verbin H, et al. Optic nerve transection in monkeys may result in secondary degeneration of retinal ganglion cells. Invest Ophthalmol Vis Sci. 2001; 42:975–982. [PubMed: 11274074]

Levkovitch-Verbin H, et al. A model to study differences between primary and secondary degeneration of retinal ganglion cells in rats by partial optic nerve transection. Invest Ophthalmol Vis Sci. 2003; 44:3388–3393. [PubMed: 12882786]

Levy NS. The effects of elevated intraocular pressure on slow axonal protein flow. Invest Ophthalmol. 1974; 13:691–695. [PubMed: 4137262]

Liang Y, et al. Impact of systemic blood pressure on the relationship between intraocular pressure and blood flow in the optic nerve head of nonhuman primates. Invest Ophthalmol Vis Sci. 2009; 50:2154–2160. [PubMed: 19074806]

Liu X, et al. Herpes simplex virus mediated gene transfer to primate ocular tissues. Exp Eye Res. 1999; 69:385–395. [PubMed: 10504272]

Lockwood H, et al. Lamina cribrosa microarchitecture in normal monkey eyes part 1: methods and initial results. Invest Ophthalmol Vis Sci. 2015; 56:1618–1637. [PubMed: 25650423]

Luo X, et al. Relation between macular retinal ganglion cell/inner plexiform layer thickness and multifocal electroretinogram measures in experimental glaucoma. Invest Ophthalmol Vis Sci. 2014; 77:4512–4524. [PubMed: 24970256]

Masamizu Y, et al. Local and retrograde gene transfer into primate neuronal pathways via adeno-associated virus serotype 8 and 9. Neuroscience. 2011; 193:249–258. [PubMed: 21782903]

Miller NR, et al. Sustained neuroprotection from a single intravitreal injection of PGJ(2) in a nonhuman primate model of nonarteritic anterior ischemic optic neuropathy. Invest Ophthalmol Vis Sci. 2014; 55:7047–7056. [PubMed: 25298416]

Minckler DS, et al. Orthograde and retrograde axoplasmic transport during acute ocular hypertension in the monkey. Invest. Ophthalmol. Vis. Sci. 1977; 16:426–441. [PubMed: 67096]

Minckler DS, et al. Radioautographic and cytochemical ultrastructural studies of axoplasmic transport in the monkey optic nerve head. Invest. Ophthalmol. Vis. Sci. 1978; 17:33–50. [PubMed: 74368]

Minckler DS, Tso MO. A light microscopic, autoradiographic study of axoplasmic transport in the normal rhesus optic nerve head. Am J Ophthalmol. 1976; 82:1–15. [PubMed: 59548]

Minckler DS, et al. A light microscopic, autoradiographic study of axoplasmic transport in the optic nerve head during ocular hypotony, increased intraocular pressure, and papilledema. Am J Ophthalmol. 1976; 82:741–757. [PubMed: 63246]

Morgan JE. Optic nerve head structure in glaucoma: astrocytes as mediators of axonal damage. Eye. 2000; 14:437–444. Pt 3B. [PubMed: 11026971]

Morgan JE, et al. Retinal ganglion cell death in experimental glaucoma. Br J Ophthalmol. 2000; 84:303–310. [PubMed: 10684843]

Morrison JC, et al. Aging changes of the rhesus monkey optic nerve. Invest. Ophthalmol. Vis. Sci. 1990a; 31:1623–1627. [PubMed: 2387691]

Morrison JC, et al. Optic nerve head extracellular matrix in primary optic atrophy and experimental glaucoma. Arch Ophthalmol. 1990b; 108:1020–1024. [PubMed: 2369339]

Morrison JC, et al. Structural proteins of the neonatal and adult lamina cribrosa. Arch Ophthalmol. 1989; 107:1220–1224. [PubMed: 2757553]

Nguyen JV, et al. Myelination transition zone astrocytes are constitutively phagocytic and have synuclein dependent reactivity in glaucoma. Proc Natl Acad Sci U S A. 2011

Nicolela MT, et al. Agreement among clinicians in the recognition of patterns of optic disk damage in glaucoma. Am J Ophthalmol. 2001; 132:836–844. [PubMed: 11730646]

Nork TM, et al. Serial multifocal electroretinograms during long-term elevation and reduction of intraocular pressure in non-human primates. Doc Ophthalmol. 2010; 120:273–289. [PubMed: 20422254]

Nork TM, et al. Measurement of regional choroidal blood flow in rabbits and monkeys using fluorescent microspheres. Arch Ophthalmol. 2006; 124:860–868. [PubMed: 16769840]

Nork TM, et al. Protection of ganglion cells in experimental glaucoma by retinal laser photocoagulation. Arch Ophthalmol. 2000a; 118:1242–1250. [PubMed: 10980770]

Nork TM, et al. Swelling and loss of photoreceptors in chronic human and experimental glaucomas. Arch Ophthalmol. 2000b; 118:235–245. [PubMed: 10676789]

Ogden TE. Nerve fiber layer of the macaque retina: retinotopic organization. Invest Ophthalmol Vis Sci. 1983a; 24:85–98. [PubMed: 6826318]

Ogden TE. Nerve fiber layer of the owl monkey retina: retinotopic organization. Invest Ophthalmol Vis Sci. 1983b; 24:265–269. [PubMed: 6832902]

Ogden TE. Nerve fiber layer of the primate retina: morphometric analysis. Invest Ophthalmol Vis Sci. 1984; 25:19–29. [PubMed: 6698729]

Ogden TE, Miller RF. Studies of the optic nerve of the rhesus monkey: nerve fiber spectrum and physiological properties. Vision Res. 1966; 6:485–506. [PubMed: 4976686]

Orgul S, et al. An endothelin-1-induced model of chronic optic nerve ischemia in rhesus monkeys. J Glaucoma. 1996a; 5:135–138. [PubMed: 8795746]

Orgul S, et al. An endothelin-1 induced model of optic nerve ischemia in the rabbit. Invest Ophthalmol Vis Sci. 1996b; 37:1860–1869. [PubMed: 8759355]

Palczewska G, et al. Endogenous fluorophores enable two-photon imaging of the primate eye. Invest Ophthalmol Vis Sci. 2014; 55:4438–4447. [PubMed: 24970255]

Patel NB, et al. Age-associated changes in the retinal nerve fiber layer and optic nerve head. Invest Ophthalmol Vis Sci. 2014a; 55:5134–5143. [PubMed: 25052998]

Patel NB, et al. Retinal Nerve Fiber Layer Assessment: Area versus Thickness Measurements from Elliptical Scans Centered on the Optic Nerve. Invest Ophthalmol Vis Sci. 2011; 52:2477–2489. [PubMed: 21220552]

Patel NB, et al. The relationship between retinal nerve fiber layer thickness and optic nerve head neuroretinal rim tissue in glaucoma. Invest Ophthalmol Vis Sci. 2014b; 55:6802–6816. [PubMed: 25249610]

Pazos M, et al. Rat optic nerve head anatomy within 3D histomorphometric reconstructions of normal control eyes. Exp Eye Res. 2015 First published on May 25, 2015 as doi:10.1016/j.exer.2015.05.011.

Pease ME, et al. Obstructed axonal transport of BDNF and its receptor TrkB in experimental glaucoma. Invest Ophthalmol Vis Sci. 2000; 41:764–774. [PubMed: 10711692]

Petrig BL, et al. Laser Doppler flowmetry and optic nerve head blood flow. Am J Ophthalmol. 1999; 127:413–425. [PubMed: 10218694]

Povazay B, et al. Minimum distance mapping using three-dimensional optical coherence tomography for glaucoma diagnosis. J Biomed Opt. 2007; 12:041204. [PubMed: 17867793]

Qin L, et al. Spectral Domain Optical Coherence Tomography (SDOCT) Detected Lamina Cribrosa Compliance Change in Non-human Primate (NHP) Early Experimental Glaucoma (EEG). 2013 ARVO Meeting Abstracts. 54, ARVO Abstract# 53.

Qin L, et al. Spectral Domain Optical Coherence Tomography (SDOCT) detected lamina cribrosa compliance during acute compliance testing between young and old normal Non-human Primate (NHP) eyes. Invest Ophthalmol Vis Sci. 2012 53, ARVO Abstract# 2824.

Quigley H, Anderson DR. The dynamics and location of axonal transport blockade by acute intraocular pressure elevation in primate optic nerve. Invest Ophthalmol. 1976; 15:606–616. [PubMed: 60300]

Quigley H, et al. Change in the appearance of elastin in the lamina cribrosa of glaucomatous optic nerve heads. Graefes Arch Clin Exp Ophthalmol. 1994; 232:257–261. [PubMed: 8045433]

Quigley HA. Neuronal death in glaucoma. Prog Retin Eye Res. 1999; 18:39–57. [PubMed: 9920498]

Quigley HA, Addicks EM. Chronic experimental glaucoma in primates. I. Production of elevated intraocular pressure by anterior chamber injection of autologous ghost red blood cells. Invest Ophthalmol Vis Sci. 1980a; 19:126–136. [PubMed: 6766124]

Quigley HA, Addicks EM. Chronic experimental glaucoma in primates. II. Effect of extended intraocular pressure elevation on optic nerve head and axonal transport. Invest Ophthalmol Vis Sci. 1980b; 19:137–152. [PubMed: 6153173]

Quigley HA, Addicks EM. Regional differences in the structure of the lamina cribrosa and their relation to glaucomatous optic nerve damage. Arch Ophthalmol. 1981; 99:137–143. [PubMed: 7458737]

Quigley HA, Addicks EM. Quantitative studies of retinal nerve fiber layer defects. Arch Ophthalmol. 1982; 100:807–814. [PubMed: 7082210]

Quigley HA, Anderson DR. Distribution of axonal transport blockade by acute intraocular pressure elevation in the primate optic nerve head. Invest Ophthalmol Vis Sci. 1977a; 16:640–644. [PubMed: 68942]

Quigley HA, Anderson DR. The histologic basis of optic disk pallor in experimental optic atrophy. Am J Ophthalmol. 1977b; 83:709–717. [PubMed: 405870]

Quigley HA, et al. Alterations in elastin of the optic nerve head in human and experimental glaucoma. Br J Ophthalmol. 1991a; 75:552–557. [PubMed: 1911659]

Quigley HA, et al. Larger optic nerve heads have more nerve fibers in normal monkey eyes. Arch Ophthalmol. 1991b; 109:1441–1443. [PubMed: 1929937]

Quigley HA, et al. Descending optic nerve degeneration in primates. Invest Ophthalmol Vis Sci. 1977; 16:841–849. [PubMed: 408291]

Quigley HA, et al. Quantitative study of collagen and elastin of the optic nerve head and sclera in human and experimental monkey glaucoma. Curr Eye Res. 1991c; 10:877–888. [PubMed: 1790718]

Quigley HA, et al. The mechanism of optic nerve damage in experimental acute intraocular pressure elevation. Invest Ophthalmol Vis Sci. 1980; 19:505–517. [PubMed: 6154668]

Quigley HA, et al. Blockade of rapid axonal transport. Effect of intraocular pressure elevation in primate optic nerve. Arch Ophthalmol. 1979; 97:525–531. [PubMed: 84662]

Quigley HA, et al. Blood vessels of the glaucomatous optic disc in experimental primate and human eyes. Invest Ophthalmol Vis Sci. 1984; 25:918–931. [PubMed: 6746235]

Quigley HA, et al. Optic nerve head blood flow in chronic experimental glaucoma. Arch Ophthalmol. 1985; 103:956–962. [PubMed: 4015488]

Quigley HA, et al. Retinal ganglion cell death in experimental glaucoma and after axotomy occurs by apoptosis. Invest Ophthalmol Vis Sci. 1995; 36:774–786. [PubMed: 7706025]

Radius RL. Regional specificity in anatomy at the lamina cribrosa. Arch Ophthalmol. 1981; 99:478–480. [PubMed: 7213169]

Radius RL, Anderson DR. The course of axons through the retina and optic nerve head. Arch Ophthalmol. 1979; 97:1154–1158. [PubMed: 109071]

Radius RL, Anderson DR. Breakdown of the normal optic nerve head blood-brain barrier following acute elevation of intraocular pressure in experimental animals. Invest Ophthalmol Vis Sci. 1980; 19:244–255. [PubMed: 6153639]

Radius RL, Gonzales M. Anatomy of the lamina cribrosa in human eyes. Arch Ophthalmol. 1981; 99:2159–2162. [PubMed: 7030283]

Rangaswamy NV, et al. Effect of experimental glaucoma in primates on oscillatory potentials of the slow-sequence mfERG. Invest Ophthalmol Vis Sci. 2006; 47:753–767. [PubMed: 16431977]

Reis AS, et al. Influence of clinically invisible, but optical coherence tomography detected, optic disc margin anatomy on neuroretinal rim evaluation. Invest Ophthalmol Vis Sci. 2012a; 53:1852–1860. [PubMed: 22410561]

Reis AS, et al. Optic disc margin anatomy in patients with glaucoma and normal controls with spectral domain optical coherence tomography. Ophthalmology. 2012b; 119:738–747. [PubMed: 22222150]

Ren R, et al. Anterior lamina cribrosa surface depth, age, and visual field sensitivity in the Portland Progression Project. Invest Ophthalmol Vis Sci. 2014; 55:1531–1539. [PubMed: 24474264]

Reynaud J, et al. Automated quantification of optic nerve axons in primate glaucomatous and normal eyes--method and comparison to semi-automated manual quantification. Invest Ophthalmol Vis Sci. 2012; 53:2951–2959. [PubMed: 22467571]

Roberts MD, et al. Remodeling of the connective tissue microarchitecture of the lamina cribrosa in early experimental glaucoma. Invest Ophthalmol Vis Sci. 2009; 50:681–690. [PubMed: 18806292]

Roberts MD, et al. Correlation between local stress and strain and lamina cribrosa connective tissue volume fraction in normal monkey eyes. Invest Ophthalmol Vis Sci. 2010a; 51:295–307. [PubMed: 19696175]

Roberts MD, et al. Changes in the biomechanical response of the optic nerve head in early experimental glaucoma. Invest Ophthalmol Vis Sci. 2010b; 51:5675–5684. [PubMed: 20538991]

Sanchez RM, et al. The number and diameter distribution of axons in the monkey optic nerve. Invest Ophthalmol Vis Sci. 1986; 27:1342–1350. [PubMed: 3744724]

Sandell JH, Peters A. Effects of age on nerve fibers in the rhesus monkey optic nerve. J Comp Neurol. 2001; 429:541–553. [PubMed: 11135234]

See JL, et al. Rates of neuroretinal rim and peripapillary atrophy area change: a comparative study of glaucoma patients and normal controls. Ophthalmology. 2009; 116:840–847. [PubMed: 19410941]

Sredar N, et al. 3D modeling to characterize lamina cribrosa surface and pore geometries using in vivo images from normal and glaucomatous eyes. Biomed Opt Express. 2013; 4:1153–1165. [PubMed: 23847739]

Stone J, Johnston E. The topography of primate retina: a study of the human, bushbaby, and new-and old-world monkeys. J Comp Neurol. 1981; 196:205–223. [PubMed: 7217355]

Stowell C, et al. Retinal proteomic changes following unilateral optic nerve transection and early experimental glaucoma in non-human primate eyes. Exp Eye Res. 2011; 93:13–28. [PubMed: 21530506]

Stowell C, et al. Myelin-Related Proteins Are Decreased In The Immediate Retrolaminar Optic Nerve (ON) In Non-Human Primates (NHP) In Early Experimental Glaucoma (EEG). 2014 ARVO Meeting Abstracts. 55, ARVO Abstract# 5034.

Stowell C, et al. Retinal proteomic changes under different ischemic conditions -implication of an epigenetic regulatory mechanism. Int J Physiol Pathophysiol Pharmacol. 2010; 2:148–160. [PubMed: 20740046]

Strouthidis NG, et al. Effect of acute intraocular pressure elevation on the monkey optic nerve head as detected by spectral domain optical coherence tomography. Invest Ophthalmol Vis Sci. 2011a; 52:9431–9437. [PubMed: 22058335]

Strouthidis NG, et al. Longitudinal change detected by spectral domain optical coherence tomography in the optic nerve head and peripapillary retina in experimental glaucoma. Invest Ophthalmol Vis Sci. 2011b; 52:1206–1219. [PubMed: 21217108]

Strouthidis NG, et al. A comparison of optic nerve head morphology viewed by spectral domain optical coherence tomography and by serial histology. Invest Ophthalmol Vis Sci. 2010; 51:1464–1474. [PubMed: 19875649]

Strouthidis NG, et al. Detection of optic nerve head neural canal opening within histomorphometric and spectral domain optical coherence tomography data sets. Invest Ophthalmol Vis Sci. 2009a; 50:214–223. [PubMed: 18689697]

Strouthidis NG, et al. Comparison of clinical and spectral domain optical coherence tomography optic disc margin anatomy. Invest Ophthalmol Vis Sci. 2009b; 50:4709–4718. [PubMed: 19443718]

Sugiyama K, et al. Optic nerve and peripapillary choroidal microvasculature in the primate. J Glaucoma. 1994; 3(Suppl 1):S45–54. [PubMed: 19920587]

Sun D, et al. Reversible reactivity by optic nerve astrocytes. Glia. 2013; 61:1218–1235. [PubMed: 23650091]

Takahashi E, et al. Epithelial mesenchymal transition-like phenomenon in trabecular meshwork cells. Exp Eye Res. 2014; 118:72–79. [PubMed: 24291802]

Tielsch JM, et al. A population-based evaluation of glaucoma screening: the Baltimore Eye Survey. Am J Epidemiol. 1991a; 134:1102–1110. [PubMed: 1746520]

Tielsch JM, et al. Racial variations in the prevalence of primary open-angle glaucoma. The Baltimore Eye Survey. JAMA. 1991b; 266:369–374. [PubMed: 2056646]

Toris CB, et al. Aqueous humor dynamics in inbred rhesus monkeys with naturally occurring ocular hypertension. Exp Eye Res. 2010; 91:860–865. [PubMed: 20868683]

Tso MO, et al. Is there a blood-brain barrier at the optic nerve head? Arch Ophthalmol. 1975; 93:815–825. [PubMed: 828849]

Vandenberghe LH, et al. AAV9 targets cone photoreceptors in the nonhuman primate retina. PLoS One. 2013; 8:e53463. [PubMed: 23382846]

Varma R, et al. Changes in optic disk characteristics and number of nerve fibers in experimental glaucoma. Am J Ophthalmol. 1992; 114:554–559. [PubMed: 1443015]

Vesti E, et al. Comparison of different methods for detecting glaucomatous visual field progression. Invest Ophthalmol Vis Sci. 2003; 44:3873–3879. [PubMed: 12939303]

Vilupuru AS, et al. Adaptive optics scanning laser ophthalmoscopy for in vivo imaging of lamina cribrosa. J Opt Soc Am A Opt Image Sci Vis. 2007; 24:1417–1425. [PubMed: 17429488]

Viswanathan S, et al. The photopic negative response of the macaque electroretinogram: reduction by experimental glaucoma. Invest Ophthalmol Vis Sci. 1999; 40:1124–1136. [PubMed: 10235545]

Wamsley S, et al. Vitreous glutamate concentration and axon loss in monkeys with experimental glaucoma. Arch Ophthalmol. 2005; 123:64–70. [PubMed: 15642814]

Wang L, et al. Static blood flow autoregulation in the optic nerve head in normal and experimental glaucoma. Invest Ophthalmol Vis Sci. 2014a; 55:873–880. [PubMed: 24436190]

Wang L, et al. Longitudinal alterations in the dynamic autoregulation of optic nerve head blood flow revealed in experimental glaucoma. Invest Ophthalmol Vis Sci. 2014b; 55:3509–3516. [PubMed: 24812551]

Wang L, et al. Depth of penetration of scanning laser Doppler flowmetry in the primate optic nerve. Arch Ophthalmol. 2001; 119:1810–1814. [PubMed: 11735792]

Wang L, et al. Anterior and posterior optic nerve head blood flow in nonhuman primate experimental glaucoma model measured by laser speckle imaging technique and microsphere method. Invest Ophthalmol Vis Sci. 2012; 53:8303–8309. [PubMed: 23169886]

Weber AJ, et al. Morphology of single ganglion cells in the glaucomatous primate retina. Invest. Ophthalmol. Vis. Sci. 1998; 39:2304–2320. [PubMed: 9804139]

Williams G, et al. Optic nerve head (ONH) connective tissue (CT) deformation within Non-Human Primate (NHP) eyes with moderate to severe (M/S) Experimental Glaucoma (EG). 2013 ARVO Meeting Abstracts. 54, ARVO Abstract# 2270.

Wygnanski T, et al. Comparison of ganglion cell loss and cone loss in experimental glaucoma. Am J Ophthalmol. 1995; 120:184–189. [PubMed: 7639302]

Yang D, et al. Optic neuropathy induced by experimentally reduced cerebrospinal fluid pressure in monkeys. Invest Ophthalmol Vis Sci. 2014a; 55:3067–3073. [PubMed: 24736050]

Yang H, et al. 3-D histomorphometry of the normal and early glaucomatous monkey optic nerve head: prelaminar neural tissues and cupping. Invest Ophthalmol Vis Sci. 2007a; 48:5068–5084. [PubMed: 17962459]

Yang H, et al. Physiologic intereye differences in monkey optic nerve head architecture and their relation to changes in early experimental glaucoma. Invest Ophthalmol Vis Sci. 2009a; 50:224–234. [PubMed: 18775866]

Yang H, et al. 3-D histomorphometry of the normal and early glaucomatous monkey optic nerve head: lamina cribrosa and peripapillary scleral position and thickness. Invest Ophthalmol Vis Sci. 2007b; 48:4597–4607. [PubMed: 17898283]

Yang H, et al. Deformation of the normal monkey optic nerve head connective tissue after acute IOP elevation within 3-D histomorphometric reconstructions. Invest Ophthalmol Vis Sci. 2009b; 50:5785–5799. [PubMed: 19628739]

Yang H, et al. Spectral Domain Optical Coherence Tomography (SDOCT) Detected Optic Nerve Head (ONH) Change Demonstrates Age-Related Differences in Young vs Old Monkey Early Experimental Glaucoma (EEG). 2011a ARVO Meeting Abstracts. 52, ARVO Abstract# 5921.

Yang H, et al. Age-related differences in longitudinal structural change by spectral-domain optical coherence tomography in early experimental glaucoma. Invest Ophthalmol Vis Sci. 2014b; 55:6409–6420. [PubMed: 25190652]

Yang H, et al. Eye-specific Onset and Spatial Pattern of Longitudinal Change Detected by Spectral Domain Optical Coherence Tomography (SDOCT) Sectoral Analysis in Non-human Primate (NHP) Early Experimental Glaucoma (EG). 2015

Yang H, et al. Deformation of the early glaucomatous monkey optic nerve head connective tissue after acute IOP elevation in 3-D histomorphometric reconstructions. Invest Ophthalmol Vis Sci. 2011b; 52:345–363. [PubMed: 20702834]

Yang H, et al. Posterior (outward) migration of the lamina cribrosa and early cupping in monkey experimental glaucoma. Invest Ophthalmol Vis Sci. 2011c; 52:7109–7121. [PubMed: 21715355]

Yucel YH, et al. Memantine protects neurons from shrinkage in the lateral geniculate nucleus in experimental glaucoma. Arch Ophthalmol. 2006; 124:217–225. [PubMed: 16476892]

Yucel YH, et al. Loss of neurons in magnocellular and parvocellular layers of the lateral geniculate nucleus in glaucoma. Arch Ophthalmol. 2000; 118:378–384. [PubMed: 10721961]

Yucel YH, et al. Atrophy of relay neurons in magno-and parvocellular layers in the lateral geniculate nucleus in experimental glaucoma. Invest Ophthalmol Vis Sci. 2001; 42:3216–3222. [PubMed: 11726625]

Zhang L, et al. Quantitative Proteomic Analysis Of Non-Human Primate (NHP) Optic Nerve (ON) In Early Experimental Glaucoma (EEG). 2014 ARVO Meeting Abstracts. 55, ARVO Abstract# 4519.

Zhi Z, et al. Impact of intraocular pressure on changes of blood flow in the retina, choroid, and optic nerve head in rats investigated by optical microangiography. Biomed Opt Express. 2012; 3:2220–2233. [PubMed: 23024915]

Zimmerman LE, et al. Pathology of the optic nerve in experimental acute glaucoma. Invest Ophthalmol. 1967; 6:109–125. [PubMed: 4225689]

1) Summarizes current strengths and weaknesses of the NHP experimental glaucoma model

2) Model History, Methods, Important Findings and Alternative Models are discussed

3) Ideas for Model Improvement and Important Next Questions are addressed

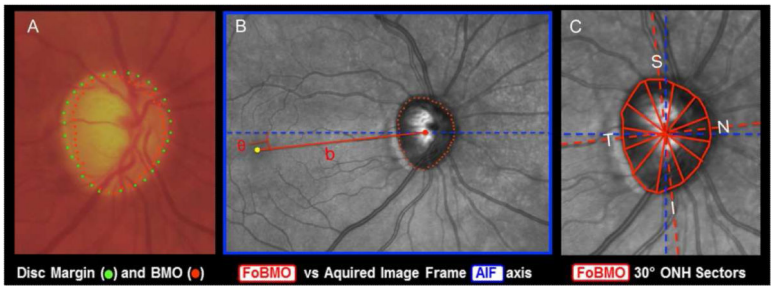

Figure 1. OCT Phenotyping in the NHP EG Model Part 1: BMO and FoBMO Axis Anatomy vs the Clinical Disc Margin and the Acquired Image Frame

(A) While in the NHP eye, OCT-detected Bruch's Membrane Opening (BMO – red points) can be the same as the clinically visible Disc Margin (green points) (Strouthidis et al., 2009b), BMO can also be regionally invisible and anatomically different from the Disc Margin (Reis et al., 2012b; Strouthidis et al., 2009b). **(B)** The Foveal –BMO centroid (FoBMO) (red) vs *Acquired Image Frame* (**AIF** - blue) Temporal-Nasal axis (He et al., 2014a). **(C)** FoBMO ONH 30° sectors.(He et al., 2014a) By colocal izing all forms of fundus imaging to the infrared image acquired at the time of OCT data set acquisition, FoBMO axis anatomy and regionalization can be superimposed upon all in-vivo and post-mortem data sets (Lockwood et al., 2015). Digitally converting all left eye data sets into right eye (OD) configuration (Lockwood et al., 2015), and using FoBMO regionalization allows the most anatomically consistent EG vs. control eye comparisons within and between animals.

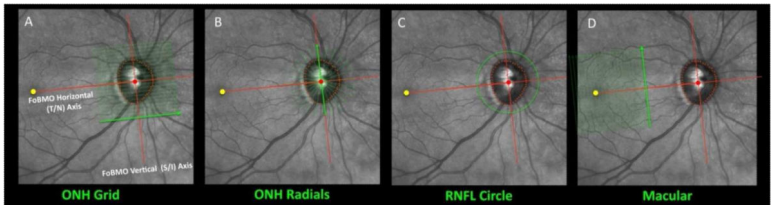

Figure 2. OCT Phenotyping in the NHP EG Model - Part 2: Acquisition of ONH, RNFL and Macula data sets relative to the Foveal-BMO Axis

OCT acquisition software now exists that utilizes eye-tracking technology (Helb et al., 2010) to automatically acquire ONH, **(A** and **B)** RNFL **(C)** and macula **(D)** images (datasets) relative to the SDOCT-detected FoBMO axis. This anatomy is determined the first time an eye is imaged and each A-scan of each subsequent scan (of the same scan type) are acquired in the same location. If an OCT device is utilized that does not have these features, post-hoc assignment of FoBMO anatomy and ONH regionalization can be accomplished (He et al., 2014a; He et al., 2014b; Lockwood et al., 2015). In our work we have chosen to emphasize radial B-scan data sets for the ONH (B) because we have shown it to efficiently capture ONH anatomy within 3D HMRNs and, in avoiding interpolation, allows improved signal to noise ratio through averaging 9 to 100 repetitions of each B-scan. This image has appeared in a previous publication (Burgoyne, 2015) and is used with permission of the publisher.

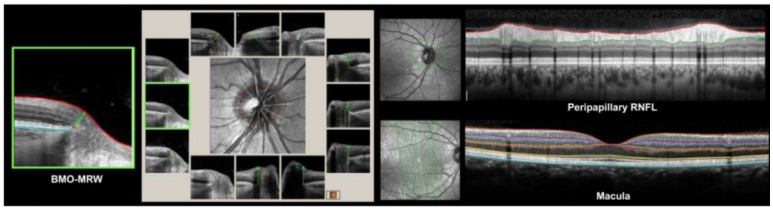

Figure 3. OCT Phenotyping in the NHP EG Model - Part 3: Automated and manually-corrected *segmentation* for the ONH rim (left and middle), RNFL (upper right) and Macula (lower right)

A large literature now supports the concept of a minimum rim measurement made from BMO in humans and NHPs (Chen, 2009; He et al., 2014a; He et al., 2014b; Patel et al., 2014a; Patel et al., 2014b; Povazay et al., 2007; Strouthidis et al., 2011b; Yang et al., 2014b). The logic for this approach has also been articulated (Chauhan and Burgoyne, 2013; Chauhan et al., 2013; Reis et al., 2012a). Several OCT manufacturers are now automatically segmented BMO-MRW (left, and by clinical clock-hour - left middle), peripapillary RNFL (upper right) and macula (lower right) anatomy which can then be manually corrected and exported for analysis.

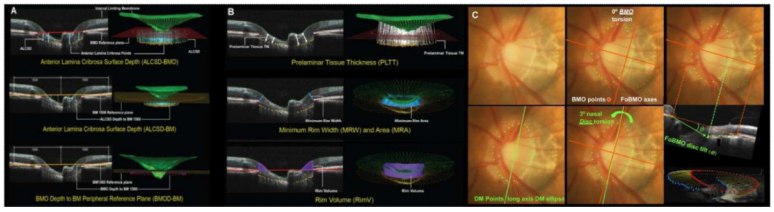

Figure 4. OCT Phenotyping in the NHP EG Model - Part 4: Phenotyping the Deep ONH will Include Quantification of ONH *Tilt*, *Torsion* and the *Neural Canal Minimum*

We and others have published extensively on a group of ONH parameters ((A) and (B)) (Gardiner et al., 2014; He et al., 2014a; He et al., 2014b; Patel et al., 2014b; Ren et al., 2014; Strouthidis et al., 2011b; Yang et al., 2014b). OCT definitions of ONH torsion and tilt are evolving (Hosseini et al., 2013; Lamparter et al., 2013). In our work, *ONH torsion* will be defined as the angle of the long axis of the disc margin ellipse relative to the vertical FoBMO axis ((C) - lower center). *BMO torsion* will be defined as the angle of the long axis of the BMO ellipse relative to the FoBMO vertical axis (shown as zero in (C - upper middle) because BMO is a circle). *ONH tilt* will be defined as the angle between a line connecting the nasal BMO point and the temporal SDOCT projection of the Disc Margin (DM) within the FoBMO B-scan (C – lower right). The *neural canal minimum* defines the smallest cross-sectional area through which the RGC axons pass using all BMO (red) and anterior scleral canal opening (blue) points (lower right) (Strouthidis et al., 2010; Strouthidis et al., 2009b). This image has appeared in a previous publication (Burgoyne, 2015) and is used with permission of the publisher.

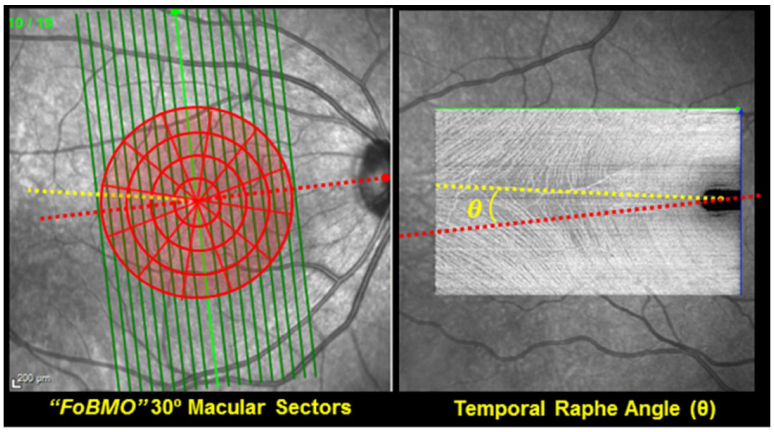

Figure 5. OCT Phenotyping in the NHP EG Model - Part 5: Phenotyping the Macula

Automated Segmentation is available to make the following thickness measurements on most instruments: Nerve Fiber Layer (NFL), RGC complex (defined to be the distance between the internal limiting membrane (ILM) and the outer nuclear layer), RGC layer (RGC cell thickness, alone) and retinal thickness (ILM to Bruch's membrane thickness). When high density grid scans are obtained, the temporal raphe can be identified within *"enface"* (C-scan) views of the NFL(Chauhan et al., 2014b) (right). The effect of using the temporal raphe versus the FoBMO axis as the "midline" for macula regionalization as well as multiple regionalization schemes (30° sectors & 500 micron intervals are shown - left) should be explored.

Table 1

Abbreviations, Acronyms and Definitions

Abbreviation	Meaning
3D HMRN	3D Histomorphometric Reconstruction
AIF	Acquired Image Frame
AION	Anterior Ischemic Optic Neuropathy
ALT	Argon Laser Trabeculoplasty
BM	Bruch's Membrane
BMO	Bruch's Membrane Opening
BP	Blood Pressure
CSF	Cerebrospinal Fluid
CSLO	Confocal Scanning Laser Ophthalmoscopy
CSLT	Confocal Scanning Laser Tomography
CT	Computed Tomography
ECM	Extracellular Matrix
EG	Experimental Glaucoma
ERG	Electroretinography
FEM	Finite Element Modeling
FoBMO	Foveal to Bruch's Membrane Opening Centroid
IACUC	International Animal Care and Use Committee
ILM	Internal Limiting Membrane
IOP	Intraocular Pressure
mfERG	Multifocal Electroretinography
MRI	Magnetic Resonance Imaging
NFL	Nerve Fiber Layer
NHP	Non-human Primate
OCT	Optical Coherence Tomography
ONH	Optic Nerve Head
PET	Positron Emission Tomography
PID	Physiologic Inter-Eye Difference
PIPD	Physiologic Inter-Eye Percent Difference
POAG	Primary Open Angle Glaucoma
Pre-EG	The EG eye prior to being lasered
RGC	Retinal Ganglion Cell
RGCC	RGC complex
RNFL	Retinal Nerve Fiber Layer
RNFLT	Retinal Nerve Fiber Layer Thickness
SBF-EM	Scanning Block Face Electron Microscopy
SDOCT	Spectral Domain Optical Coherence Tomography
SEM	Scanning Electron Microscopy

Abbreviation	Meaning
SLP	Scanning Laser Polarimetry
TCA	Topographic Change Analysis
TEM	Transmission Electron Microscopy